Ocean Engineering 126 (2016) 57–80

Contents lists available at ScienceDirect

Ocean Engineering

journal homepage: www.elsevier.com/locate/oceaneng

Review

Vortex shedding suppression and wake control: A review

Saman Rashidi [a], Masoud Hayatdavoodi [b], Javad Abolfazli Esfahani [a,*]

[a] Department of Mechanical Engineering, Ferdowsi University of Mashhad, Mashhad 91775-1111, Iran
[b] Division of Civil Engineering, School of Science and Engineering, University of Dundee, Dundee DD1 4HN, UK

ARTICLE INFO

Article history:
Received 31 December 2015
Received in revised form
19 July 2016
Accepted 27 August 2016

Keywords:
Suppression of vortex shedding
Bluff bodies
Wake control
Computational fluid dynamics
Experimental and analytical techniques

ABSTRACT

Wake destructive behavior and vortex shedding behind bluff bodies may be controlled by use of active and passive methods. Computational fluid dynamics, experimental and analytical techniques have been utilized to study this problem. In this survey, existing studies on different methods of controlling the wake destructive behavior and suppression of vortex shedding behind bluff bodies are discussed, including the very recent developments. These methods are classified into two groups. In the first group, these methods are discussed according to the type of external source or modification of the geometry of bluff body for controlling the flow. In the second group, the methods are classified according to the part of the flow, boundary layer or wake, that is modified by the method. Advantages, limitations, energy efficiency, and particular applications of each method are discussed and summarized, followed by some conclusions and recommendations. Moreover, the effectiveness of each technique on the drag reduction is discussed.

Contents

1. Introduction

Studies on wake structure and vortex shedding behind bluff bodies and analysis of flow separation have been a topic of interest

* Corresponding author.
E-mail address: abolfazl@um.ac.ir (J.A. Esfahani).

http://dx.doi.org/10.1016/j.oceaneng.2016.08.031
0029-8018/

due to their fundamental significance and practical importance in aerodynamics and hydrodynamics applications. Examples of such applications are vibration of pipelines lying on the seabottom under the influence of currents and waves, bridges, interaction of currents and waves with offshore structures, flow tubular or tube banks heat exchangers, skyscrapers, chimneystacks, suspension bridges and chimneys near tall buildings, structures in the atmospheric boundary layers and submarine pipe, see e.g., Zang et al. (2013), Zang and Gao (2014), Bovand et al. (2015a), Rashidi et al. (2014a) and Rashidi et al. (2015a). In such applications, bluff bodies experience unsteady loads due to the flow separation and formation of the wake region and vortices, which in some cases, play an important role on their design. Control of wake structures and flow separations in such cases can significantly decrease the unsteady forces on the structure; resulting in less structural vibrations. Also, the offshore industry is particularly concerned with the vortex induced vibration suppression due to the failure of components of offshore structures, like risers and spars, which leads to catastrophic environmental and economic consequences.

There are various methods to control the wake structure and vortex shedding, such as employing an external small element, modifying geometry of the obstacle (by placing tabs or streaks on the obstacle), injection and suction in porous surface, and surface roughness elements. These methods have been introduced and discussed by researchers in the past decades, however, to the author's knowledge, there has not been any attempt to classify these techniques. For example, Zdravkovich (1981) performed a review on various aerodynamic and hydrodynamic means for suppressing vortex shedding, and classified these approaches in three categorie: surface protrusions, shrouds and near wake stabilizers. The various aerodynamic and hydrodynamic means have been highlighted in this paper rather than various techniques in this field. Also, Zdravkovich (1981) reviewed different means for suppressing the vortex shedding behind circular obstacle, while other shapes, such as square, diamond, triangular, trapezius, etc. did not receive any attention. Gad-el-Hak and Bushnell (1991) performed a review on separation control. There are several control techniques that the wake characteristics are modified directly, but in paper of Gad-el-Hak and Bushnell (1991), attentions are focused on boundary layer control. In addition, many new devices and approaches are introduced after 1991. Williamson (1996) reviewed new developments and the discoveries of several new phenomena of vortex dynamics. Overview of vortex shedding regimes, 3D vortex patterns in different regimes including the laminar, transition, and higher Reynolds number regimes, wave interactions in the far wake, and 3D effects in other wake flows were also reviewed by Williamson (1996), Modi (1997) and King (1997) performed a review on moving surface boundary-layer control and vortex shedding, respectively. Williamson and Govardhan (2004) reviewed the fundamental results and discoveries on vortex-induced vibration. Free and forced vibrations of a cylinder are presented separately in their review. In another research, Kumar et al. (2008) classified recent patents on passive control techniques for vortex-induced vibrations. Choi et al. (2008) performed a review study about control of flow over the bluff bodies. However, this paper is published in the year 2008 and this means that the recent developments in this field are not covered by this paper. Moreover, some important factors about this topic such as energy efficiency of control methods and the effectiveness of each technique on the drag reduction should be highlighted with more details. These factors are necessary for assessing different control techniques. Shmilovich and Yadlin (2011) investigated flow control techniques for transport aircraft.

It appears that the literature lacks from a comprehensive study on classification of different methods for control of wake destructive behavior and suppression of vortex shedding behind bluff bodies. The current study focuses on this goal. In Section 2, a classification of various methods for controlling the wake destructive behavior and suppression of vortex shedding is provided. Section 3 presents some conclusions and suggestions based on the literature review.

2. Classification of various methods

In this study, we classify the existing aerodynamic and hydrodynamic methods used to control the wake destructive behavior and suppress the vortex shedding into nine categories. These methods are summarized below.

a) Control of vortex shedding by electrical methods
b) Control of vortex shedding by utilizing an external small element
c) Control of vortex shedding by feedback control methods
d) Control of vortex shedding by use of a magnetic field (MHD)
e) Control of vortex shedding by rotary oscillations
f) Control of vortex shedding by generating a secondary flow (suction, blowing, bleed and synthetic jets)
g) Control of vortex shedding by surface roughness
h) Control of vortex shedding by use of thermal effects
i) Control of vortex shedding by other methods

These approaches can be classified as passive and active control methods. The passive control techniques are dependent on modifications of the bluff body geometry, which affect the formation of the vortex shedding. These passive methods, class b and g, do not need any external energy during application and have a simpler implementation, which favor them over the active techniques for engineering applications. Active control methods, class a, c-f, and h, need external energy to affect the fluid flow. Another classification of these methods is based on the parts of flow that are modified in control process: the boundary layer control methods and the wake control (Choi et al., 2008). For the former method, the boundary-layer flow characteristics are changed by using the control method but the wake characteristics are modified directly by using the later control method. Next, we will introduce and discuss each method in detail.

2.1. Active control methods (energy consuming)

2.1.1. Control of vortex shedding by electrical methods (EHD)

This method is classified as active and boundary layer control method. In this method, an electric discharge creates an electric force acting on fluid particles, resulting in a change in the fluid velocity field. This force leads to a delay in separation of the flow in the trailing side of the obstacle. The ions in the fluid flow, used in this method, are created by an electrical discharge in an otherwise electrically neutral fluid. The ions are under the action of columbic forces due to the electrode of opposite sign and this leads to exchange momentum with the neutral fluid particles. This method is suitable for aerodynamic applications such as airfoils typically used in wind turbine blades, civil air traffic projects and aircraft. Fig. 1 shows the surface plasma generated to modify the flow over a circular cylinder. Fig. 2 shows a smoke visualization of plasma actuation on flow surrounding a 2-D circular cylinder at $Re = 1.8 \times 10^4$, with and without plasma actuation. It is observed that the EHD method reduces the re-circulated smoke, resulting in Karman vortex shedding suppresses.

This method is used by Artana et al. (2003) to experimentally control the near-wake flow around a circular obstacle with electrohydrodynamic actuators for Reynolds number range of $2.3 \times 10^3 < Re < 5.8 \times 10^4$. In these experiments, two electrodes

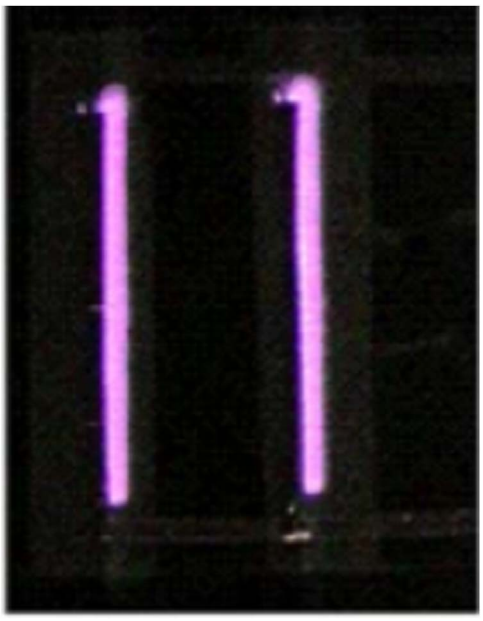

Fig. 1. Surface plasma generated to modify the flow over a circular cylinder (Figure reprinted from Sung et al. (2006) with permission from the publisher).

were flush-mounted on the obstacle wall and were charged with DC power supplies to produce a plasma sheet contouring the body. The discharge electrodes modify the shear stresses of the fluid layers increase and the base pressure increases by creating the electric force, modifying the size of the mean recirculation region. Most of the studies focusing on this method are conducted experimentally and are for a specific range of Reynolds number flow.

Hyun and Chun (2003) performed an experimental study on the wake flow control behind a circular obstacle using ion wind for Reynolds number range of $4.0\times10^3<\mathrm{Re}<8.0\times10^3$. It was found that presence of ion wind could affect the wake structure behind an obstacle significantly. Also, it was shown that the pressure drag decreases by superimposing ion wind. Control of flow separation from an airfoil (NACA 66_3-018) on high angle of attack was studied by Post and Corke (2004) using plasma actuators for Reynolds number range of $7.7\times10^4<\mathrm{Re}<3.33\times10^5$. In this study, two types of plasma actuators were utilized. The first type creates a spanwise array of streamwise vortices, and the second type creates a 2-D jet in the flow direction along the airfoil wall. These actuators were placed at the leading edge of the airfoil. It was found that the reattached flow created by the actuator leads to a decrease in drag and significant suction-pressure recovery.

In the experiments conducted by Sung et al. (2006), flow over circular obstacles was modified by plasma actuation for the Reynolds number range of $1.0\times10^4<\mathrm{Re}<4.0\times10^4$. A PIV technique was applied to quantify the changes in the wake structure. It was shown that modest discharge power into the boundary layer, created by a dielectric barrier discharge, can decrease the wake momentum deficit significantly by influencing flow separation. Less recirculation was observed in the recirculation region when the plasma is actuated. Thomas et al. (2008) used plasma actuators for the cylinder flow control and noise reduction. Both steady and unsteady actuation were used in the experiments for $\mathrm{Re}=3.3\times10^4$. It was shown that steady actuation is more suitable for noise-control applications; the unsteady actuation is affected by an unsteady body force and creates a tone at the actuation frequency. Note that there is a less power dissipation for each actuator for unsteady actuation due to a lower duty cycle. Chaos controlling is referred to the stabilization of unstable periodic orbits by means of small system perturbations. It is widely used in general non-linear dynamics problems. Muddada and Patnaik (2011) reviewed some chaos control strategies and discussed their relevance to some fluid turbulence applications. Through a computational study, vortex shedding behind a blunt trailing edge was controlled experimentally using plasma actuators by Nati et al. (2013). They focused on laminar boundary layer regime on an elongated D-shaped flat plate of 12 mm thickness with a free-stream velocity of 10 m/s. Their results show that the vortex shedding frequency peak is decreased during the steady plasma actuation by 10 dB.

Finally, this method is classified as active and boundary layer control method. In this method, the electrodes create electric force acting on fluid particles, resulting in a change in the fluid velocity field. This force leads to a delay in separation of the flow in the trailing side of the obstacle. As mentioned by e.g. Artana et al. (2003), it is more efficient to mount the electrodes on the surface of the bluff bodies because most of the momentum should be transferred in fluid layers that have a very low kinetic energy. This leads to important changes in the fluid dynamics with minimum power added to the flow. EHD mitigates some of the drawbacks of active flow control methods. This method has some favorable features as an active flow control such as low power consumption, simple construction, robustness, and high frequency response. Moreover, the electric discharge varies in space and time and so creates an easy changeable force. The electric discharge can be employed only when needed, and when not in use, they have no destructive effects.

Table 1 summarizes researches on application of EHD to control the vortex shedding behind a bluff body. As shown in this table, these researches have covered only flows with moderate Reynolds number. More studies are necessary for higher range of Reynolds numbers (i.e. $\mathrm{Re}>10^5$). All studies for this method are performed in air. Application of this method in ocean engineering, with water

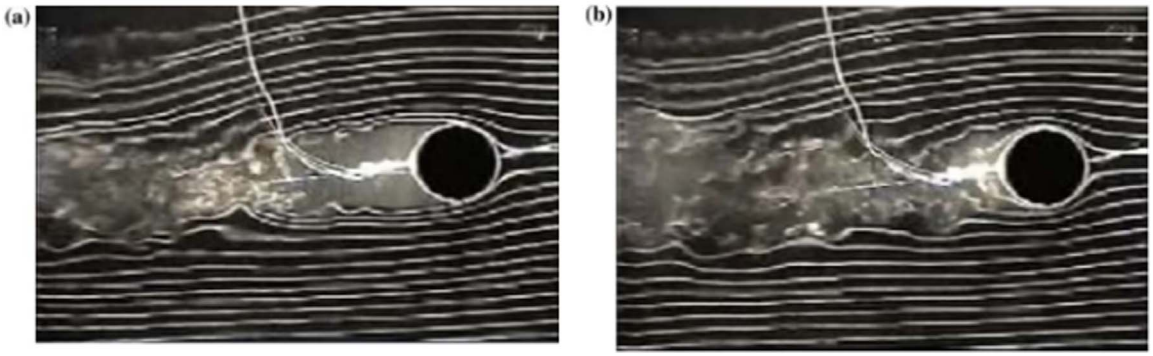

Fig. 2. Smoke visualization of plasma actuation on flow surrounding a circular cylinder at $\mathrm{Re}=1.8\times10^4$ for two cases of (a) with and (b) without plasma actuation (Flow is from right to left; Figure reprinted from Sung et al. (2006) with permission from the publisher).

Table 1
Researches on application of EHD to control the vortex shedding behind a bluff body.

Authors	Type of research	Type of fluid	Reynolds number
Artana et al. (2003)	Experimental	air	2.3×10^3–5.8×10^4
Hyun and Chun (2003)	Experimental	air	4.0×10^3–8.0×10^3
Post and Corke (2004)	Experimental	air	7.7×10^4–3.3×10^5
Sung et al. (2006)	Experimental	air	1.0×10^4–4.0×10^4
Thomas et al. (2008)	Experimental	air	3.3×10^4
Nati et al. (2013)	Experimental	air	3.8×10^3–7.3×10^3

being as fluid, is questionable. The results show a lack of information about application of numerical approaches in this method. However, vortex induced vibration phenomenon is observed in slender flexible structures as a destructive aerodynamic excitation. Studies on the control of the flows with this phenomenon by EHD method have remained interesting.

2.1.2. Control of vortex shedding by feedback control methods

This method is classified as active and wake control method. It is possible to apply feedback from a suitable sensor to an actuator for stabilizing the wake and suppressing the vortex shedding at Reynolds numbers close to the onset of vortex shedding, see e.g. Park et al. (1994). In this method, the control input is modified successively according to the response of the flow system. This method is widely used in aircraft and projectile aerodynamics including dynamic stall control, marine structures, chemical mixing improvement, submarine periscopes, increase mixing and heat transfer in combustion. A sample set up of this control method is shown in Fig. 3. The localized cross-stream velocity measurement in the cylinder wake region is feedback to the compensator, R(s), which drives the cylinder rotation. The actuation is understood by unsteady angular rotations of the circular obstacle surface φ(t).

Feedback control method can be used to control the wake and vortex shedding behind a bluff body. For example, Williams and Zhao (1989) presented an active experimental method for controlling the vortex shedding behind a circular obstacle at $Re=4.0\times10^2$, sending acoustic feedback signals. These signals were taken from hot-wires in the wake of the obstacle. The shedding was suppressed by switching on the controller after two or three vortex shedding periods. Tao et al. (1996) experimentally presented a feedback control method to suppress and excite the vortex shedding behind a circular obstacle. The feedback perturbations were created inside the wake by oscillating the obstacle transversely to the ongoing flow. They observed that the peaks at the vortex shedding frequency decrease under the feedback suppression. Roussopoulos and Monkewitz (1996) proposed a nonlinear model for vortex shedding control in cylinder wakes. They used the feedback control of Karman vortex shedding for critical value of Re ~ 47. It was observed that the vortex shedding is suppressed only at the spanwise location of the sensor for long cylinders. Fujisawa et al. (2001) controlled experimentally the vortex shedding behind a circular obstacle at moderate Reynolds numbers. They used a rotary cylinder oscillations controlled by the feedback signal of a reference velocity in the main obstacle. They showed that the fluid forces and the velocity fluctuations decreases by the feedback control with optimum values of the phase lag and feedback gain. The feedback gain is the ratio of the maximum of the circumferential velocity of the cylinder to the maximum filtered reference velocity, and the phase lag is defined as the time lag in degrees between the filtered velocity signal and the monitored angular velocity signal.

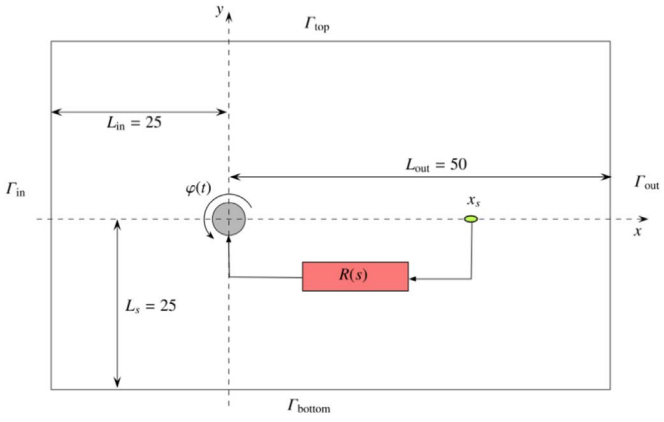

Fig. 3. A sample set up of a feedback control method (Flow is from left to right; Figure reprinted from Carini et al. (2015) with permission from the publisher).

Fujisawa and Nakabayashi (2002) experimentally controlled the vortex shedding behind a circular obstacle by the rotational feedback oscillations. They used the neural network approach for calculating the optimum condition. Their results showed that the drag force is decreased by about 16% and the lift force is suppressed about 70% in comparison with the stationary obstacle. Wolfe and Ziada (2003) performed an experimental study on the effect of feedback control on the vortex shedding behind two tandem obstacles in cross-flow. The aim of this study was to decrease the downstream obstacle response to vortex shedding and turbulence excitations. Feedback control is utilized for resonant and non-resonant cases. Frequency of vortex shedding coincides with the resonance frequency of the downstream obstacle for resonant case, but the shedding frequency is about 30% higher than the downstream obstacle resonance frequency for non-resonant case. They observed that the feedback control can significantly decrease the downstream obstacle response to turbulence excitations and vortex shedding. Leclerc et al. (2006) presented a numerical feedback control method for controlling the laminar vortex shedding behind a circular obstacle due to a compressible flow. This method was based on the incomplete sensitivities and gradient evaluation by complex variable method. Muddada and Patnaik (2010) proposed an algorithm to model and control vortex shedding behind a circular obstacle. Multiple-feedback sensors, actuators and a control strategy are used in this approach. The state of the flow is reported by some sensors that are located in the downstream of the body. Two external actuators are used to control the fluid flow. The actuators respond with a rotation parameter that this parameter temporally varies by the control algorithm. They considered the range of $Re=1.0\times10^2$–3.0×10^2. They observed that the wake gradually becomes weaker and the vortex shedding completely suppresses for higher rotation rate of the control cylinders. Lu et al. (2011) was able to reduce the lift force on a circular cylinder by about 50% at low Reynolds number, using the feedback rotary oscillation method. Carini et al. (2015) presented a linear feedback control for the unsteady cylinder wake at low Reynolds numbers. The classical small-gain has been used to design a full-dimensional stabilising compensator of the linearized Navier–Stokes equations. Also, they investigated the effect of sensor placement on the compensator performance. It was found that the amount of control energy for stabilizing the flow characteristics by a small, lower plateau for $11 < x_s < 14$ when the sensor is moved along the flow centerline, where x_s is the streamwise locations of the sensor in the far-wake region, see the green elliptic in Fig. 3.

There is a feedback control method called linear Proportional Integral Differential (PID) control. In this control method, only the output is available and used for feedback. Fig. 4 shows a block diagram of the PID control. It should be noted that the controller is a combination of a simple gain (P control), an integrator (I control), a differentiator (D control) or some weighted combination of these

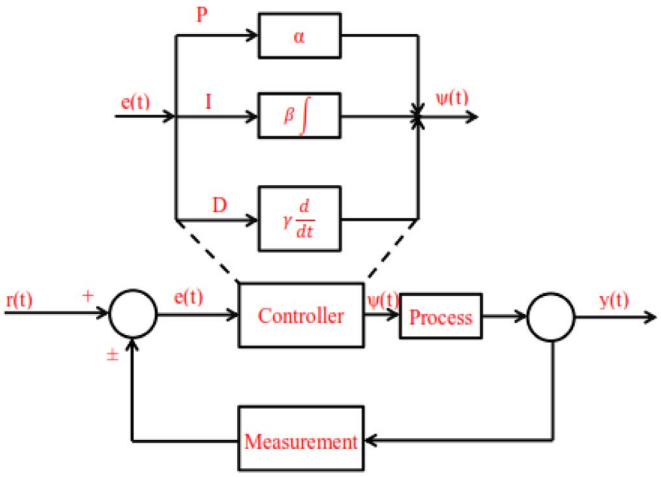

Fig. 4. Block diagram of the PID control, see e.g. Son et al. (2011).

possibilities, see e.g. Son et al. (2011).

In this figure, ψ(t), e(t) α, β and γ are the control input, error, proportional, integral and differential gains, respectively. Moreover, r and y indicate the reference input (or desired response) and process output, respectively. Son et al. (2011) summarized the researches on the application of the PID control to annihilate the vortex shedding behind a bluff body. The results of these researches are presented in Table 2. The ranges of Reynolds number, actuation type and feedback law (P control, P control with phase shift, PI and PID) for each research are presented in this table.

From these studies, Son et al. (2011) concluded that the P controls are very sensitive to the amount of phase shift and sensing position. Therefore, P controls may be used as an effective method to suppress the vortex shedding or decrease its strength by considering suitable values for these variables. Son et al. (2011) also concluded that the reductions in velocity fluctuations in the wake and the strength of vortex shedding are intensified with increase in the proportional gain. However, a large gain leads to more system instability. As shown in this table, the research of Zhang et al. (2004) is the only study where the PI and PID controls are utilized to control the flow over a bluff body. They decreased both the cylinder vibration amplitude and streamwise velocity fluctuations by PID controls.

Son et al. (2011) utilized the P, PI and PD to control the flow over a circular cylinder for the Reynolds numbers of 60 and 1.0×10^2. They measured the transverse velocity at a centreline position in the wake for sensing, and determined the actuation velocity from the P, PI or PD control. They observed that the velocity, lift fluctuations and the mean drag decrease by addition of a D or an I control to the P control for the cases that the P control does not completely suppress the vortex shedding.

Extremum is another feedback control method used to supress the vortex shedding by seeking control. This method is used as an online optimization technique to control the dynamic (nonlinear) systems characterized by an output extremum in a steady state. These controllers are used to find an optimal set point to modify the flow around the bluff bodies. Beaudoin et al. (2006) controlled the drag exerted on a bluff-body at large Reynolds number ($Re = 2.0 \times 10^4$) by extremum-seeking control. The set point in this study was defined as the minimum cost of global energy consumption of a turbulent separated flow (drag reduction versus actuator's energy). They used the extremum-seeking control to find the lowest value for cost of global energy consumption. They observed that the system works around its optimal state of lower energy consumption by using this algorithm. Becker and King (2006) controlled the separation on a high-lift configuration by using extremum seeking control. Their results showed the capability of this method to minimize the separation even in the presence of disturbances.

Feedback method was classified as an active wake control method. With the development of Microelectromechanical systems and smart materials, intelligent sensing and actuator techniques, this method has been popular rapidly among the researchers in last years. Indeed, this method is a combinatorial method that directly modifies the wake characteristics. Note that this method is not easy to simulate even with the rapid developments in computer power and CPU. There are some numerical techniques to decrease the amount of computations. For example, it is possible to replace the Navier Stokes equation by a low order dynamical system, or to find new methods to calculate the gradient of the cost function, see e.g. Leclerc et al. (2006). We note that this is a costly method. Therefore, an energetic and optimization analyses are necessary for this method. Flow visualization is a good technique to provide an overall picture of the change in wake by using feedback control.

Table 3 provides a summary on the research conducted on application of feedback method to control the vortex shedding and flow separation of a bluff body. As presented in this table, researchers used different actuations for this method. However, it can be seen that the numerical methods have been used for only very low Reynolds number. Moreover, the potential of this method at moderate and high Reynolds numbers is very significant from an engineering viewpoint and requires future study. A relatively low cost method in this classification is application of sound field as actuation. More researches are needed about this technique as the ability, advantages and disadvantages of this technique are still unclear.

2.1.3. Control of vortex shedding by generating a secondary flow (Suction, blowing, base bleed and synthetic jets)

These methods are classified as active wake control method. It is possible to control the flow around bluff bodies by generating a secondary flow (suction, blowing, base bleed). For suction and blowing, the wall of obstacle is penetrable and the suction or blowing velocity is defined. For base bleed method, the wall of

Table 2
Previous studies of the P, PI and PID controls for flow over a cylinder, see e.g. Son et al. (2011).

Author	Reynolds number	Actuation	Feedback law
Berger (1967)	laminar	Cylinder displacement	P
Williams and Zhao (1989)	4.0×10^2	Loudspeakers	P with phase shift
Baz and Ro (1991)	1.716×10^4–2.6555×10^4	Cylinder displacement	P
Roussopoulos (1993)	50–65 and 1.2×10^2	Loudspeakers	P with phase shift
Park et al. (1994)	60 and 80	Blowing/suction	P
Warui and Fujisawa (1996)	6.7×10^3	Cylinder displacement	P with phase shift
Huang (1996)	4.95×10^3, 6.5×10^3 and 1.3×10^4	Blowing/suction	P with phase shift
Zhang et al. (2004)	3.5×10^3	Cylinder displacement	P, PI, PID
Hiejima et al. (2005)	2.0×10^2	Blowing/suction	P with phase shift

Table 3
Researches on application of feedback method to control the vortex shedding and flow separation of a bluff body.

Author	Reynolds number	Actuation	Spatial dimensions	Type of research	Type of fluid
Williams and Zhao (1989)	4.0×10^2	Loudspeakers	–	Experimental	Air
Roussopoulos and Monkewitz (1996)	50	Loudspeakers	2D	Numerical	–
Tao et al. (1996)	48.5 and 51	Oscillating the cylinder transverse to the on-coming flow	–	Experimental	Water
Fujisawa et al. (2001)	6.7×10^3 and 2.0×10^4	Rotary cylinder oscillations	–	Experimental	Air
Wolfe and Ziada (2003)	4.11×10^4–5.79×10^4	Synthetic jet	–	Experimental	Air
Leclerc et al. (2006)	1.0×10^2	Blowing/suction	2D	Numerical	–
Lu et al. (2011)	60–200	Rotary cylinder oscillations	2D	Numerical	–
Carini et al. (2015)	50–90	Rotations of the cylinder surface	2D	Numerical	–

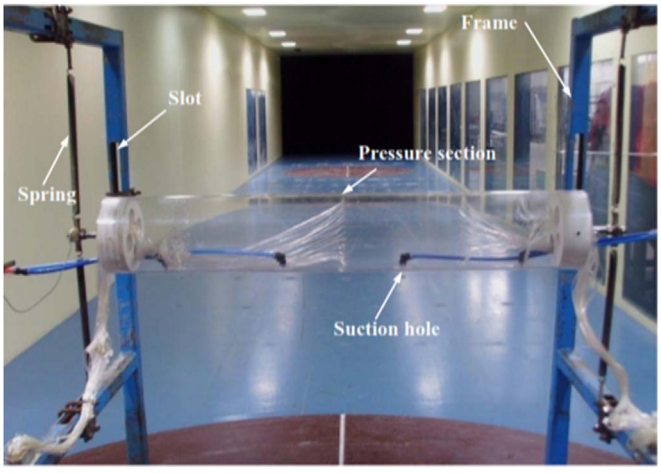

Fig. 5. Experimental setup utilized to suppress the vortex-induced vibration of a circular cylinder by using suction flow. (Figure reprinted from Chen et al. (2013) with permission from the publisher).

obstacle is not penetrable and the secondary flow is injected at the edge of obstacle. The suction, blowing and bleed are used as energy input for controlling the flow. These techniques are widely used in long-span suspension bridges and cable-stayed bridges, see e.g. Chen et al. (2013). Fig. 5 shows an experimental setup used to suppress the vortex-induced vibration of a circular cylinder by means of suction flow.

The time-averaged streamline contours with injection through the surfaces of a square cylinder for different Reynolds numbers are shown in Fig. 6. Here, Γ represents the injection parameter, defined as the ratio of the fluid velocity through the porous wall to inlet streamwise velocity. It is observed that the wake structure changes significantly when using injection; the vortices disappear for higher injection parameter. In this figure, the pressure coefficient is defined by:

$$C_p = \frac{(p_{in} - p_w)}{0.5\rho U_{in}^2} \quad (1)$$

where "in" and "w" subscripts demonstrate inlet and cylinder wall, respectively. Moreover, p and U are the pressure and velocity, respectively.

Formation of turbulent boundary layers around a cylinder by using surface suction is investigated experimentally by Seal and Smith (1999). It is shown that the surface suction leads to i) weakening the instantaneous turbulent vortex and its associated surface interactions and ii) weakening the average downstream extensions of the vortex. Delaunay and Kaiktsis (2001) studied effects of steady base suction and blowing on the stability and dynamics of the wake behind circular obstacle at low Reynolds numbers, using a numerical method. In this paper, all terms in continuity and momentum equations were discretized based on a Legendre spectral element method except the time term that was discretized based on second-order accurate mixed stiffly stable scheme. They found that slight blowing or high enough suction stabilizes the wake for supercritical Reynolds number regime ($Re > 47$). However, they observed that the wake could be destabilized for the subcritical regime by suction, whereas blowing had no detectable effect on the flow stability.

Optimal control of 2-D cylinder wakes via suction and blowing is investigated numerically by Li et al. (2003) for Reynolds numbers up to 1.1×10^2. They observed that an open-loop control can be used for suppressing the vortex shedding in the wake of a circular obstacle in a robust way. Kim and Choi (2005) investigated the distributed forcing of flow over a circular obstacle for the range of Reynolds number from 40 to 3900. The distributed forcing is found by a blowing and suction from the slots placed at upper and lower surfaces of the obstacle. The optimal conditions for maximum drag reduction are occurred for the Reynolds number of 1.0×10^2. Layek et al. (2008) numerically investigated the

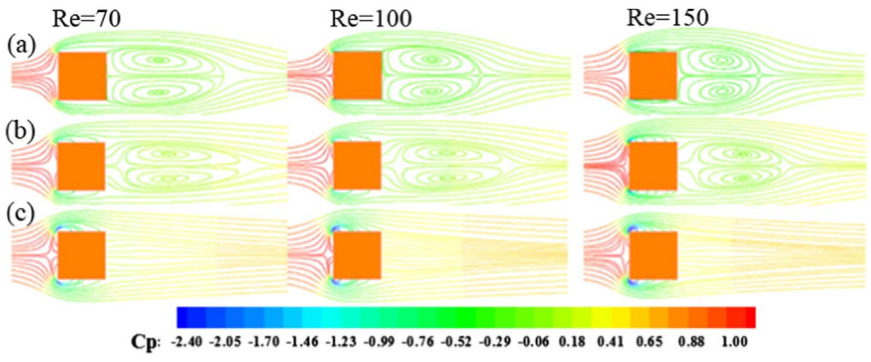

Fig. 6. Time-averaged streamlines colored by the pressure coefficient for different suction/blowing parameter and Reynolds number for case (a) without control ($|\Gamma|=0$), (b) with control ($|\Gamma|=0.05$) (c) with control ($|\Gamma|=0.15$) (Flow is from left to right; Figure reprinted from Sohankar et al. (2015) with permission from the publisher).

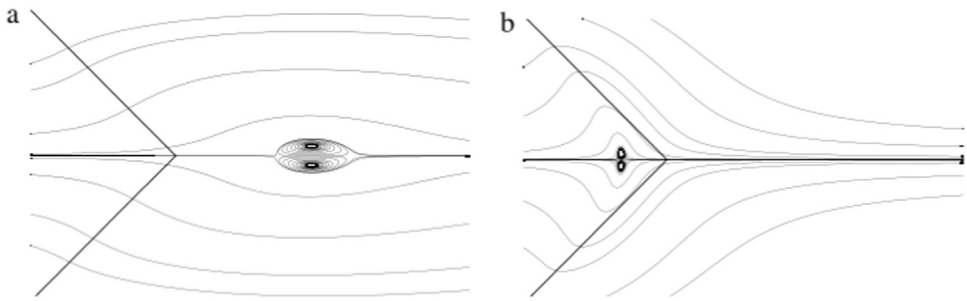

Fig. 7. Configuration of streamlines around a porous diamond obstacle for (a) Da$=1.0\times10^{-3}$ and Re$=29$; (b) Da$=1.0\times10^{-6}$ and Re$=6$ (Flow is from left to right; Figure reprinted from Valipour et al. (2014b) with permission from the publisher).

influence of suction and blowing on vortex shedding behind a square obstacle placed inside a channel. In this study, the Navier–Stokes equations were solved by a finite-difference method using staggered grid arrangement. It is concluded that the amplitude of the lift coefficient decreases by increasing the blowing velocity. Also, the flow becomes steady and symmetric for a specific value of the blowing parameter. Warjito et al. (2012) used this approach in a numerical and experimental study and modified turbulent flow structure around Ahmed's body suction flow, resulting in a reduction of the drag force by about 15%. It was shown that, using the suction in the rear part of the model results in a reduction of the wake and vortex formation. Chen et al. (2013) conducted experiments on suppression of the vortex-induced vibration of a circular obstacle by using a suction flow method. Four different steady suction flow rates were used in this study. Following this approach, they were able to decrease the amplitude of the oscillation, fluctuating wall pressure, and the unsteady aerodynamic forces acting on the obstacle. A given suction flow rate was found to optimize the control. Sohankar et al. (2015) numerically controlled fluid flow and heat transfer around a square obstacle by uniform suction and blowing at low Reynolds numbers (Re$=70-1.5\times10^2$). They considered three cases for the location of the blowing and suction, including the front surface, rear surface and top/bottom surface. They found that when the suction is employed on the top and bottom surfaces, and blowing is applied on the front and rear faces, optimum control can be achieved. Also, their study showed that the drag and lift fluctuations for the optimum configuration decrease and the maximum deduction in drag force are 61%, 67% and 72% for Re$=70$, 1.0×10^2, 1.5×10^2, respectively.

In addition, synthetic jet (unsteady blowing) is used in some cases to control the flow and separation phenomena. For example, Tensi et al. (2002) performed experimental tests to control the flow around an obstacle by synthetic jet (unsteady blowing) through a single slot disposed on the surface of the obstacle for Re$=1.05\times10^2$. The effects of this jet on delaying separation and modifying the drag coefficient were investigated through a series of experiments. It was suggested that zero-mass-flux actuator types, which require little energy, could be used for further flow control around various bodies including airfoils. Effect of novel synthetic jet on wake vortex shedding modes of a circular cylinder is investigated experimentally by Feng et al. (2010). They found that the control effect of the synthetic jet upon the flow around a circular obstacle can increase with an increase in the suction duty cycle factor, i.e., the ratio between the time duration of the suction cycle and the blowing cycle of the actuator signal and increase in the momentum coefficient. Feng and Wang (2010, 2011) experimentally controlled vortex-synchronization behind a circular obstacle with a synthetic jet positioned at the rear stagnation point at Re$=9.5\times10^2$. They observed that the symmetric shedding mode weakens the interaction between the upper and lower wake vortices and decreases turbulent kinetic energy produced by the vortices. Also, this mode has an influence on the velocity fluctuations. Joseph et al. (2013) performed an experimental flow control on the Ahmed body using micro-electro mechanical system (MEMS) pulsed micro jets. They found that the drag reduction (up to 10%) is occurred with using the micro-jets located upstream the recirculation wake created over the rear slant of the body. Chaligné et al. (2014) controlled the wake-flow behind a 2-D square obstacle by a fluidic control system. This system is made of pulsed jets placed at the upper edge of the model. This method can modify the wake flow development and the static pressure distribution around the obstacle. Liu and Feng (2015) numerically suppressed the lift fluctuations on a circular obstacle by two synthetic jets for Re$=5.0\times10^2$. In this study, the unsteady Navier–Stokes equations were solved by utilizing a finite volume method. These jets were placed at the mean separation points. They focused on reduction of the lift fluctuations by changing the vortex shedding mode. Their results showed that the complete suppression of lift fluctuations can be achieved when the typical Karman type vortex shedding are converted into the symmetric shedding modes. In some cases, base bleed or base suction effects are used for controlling the physics of flow around an obstacle.

The base bleed is secondary flow that is injected at the base of the truncated plug, see e.g. Rashidi et al. (2013). The streamline contours past a porous diamond obstacle are shown in Fig. 7. As shown in Fig. 7(a), the wake is completely detached from the cylinder wall for this range of parameters (Da$=1.0\times10^{-3}$ and Re$=29$), due to the base bleed effects. In this figure, the Darcy number is defined as:

$$Da = = K/D^2 \tag{2}$$

where, K and D are the permeability of porous medium and cylinder diameter, respectively.

Also, Fig. 7(b) shows that the wake is permeated into the porous obstacle for Da$=10^{-6}$ and Re$=6$. The negative exit velocity effect (base suction) is known to be the main reason for such a phenomenon.

Fu and Rockwell (2005) experimentally controlled the vortex formation in the near wake for the shallow flow past a vertical cylinder by base bleed through a very narrow slot. They observed that the patterns of streamline topology and Reynolds stress at the bed change even by small bleed and these changes have important consequences for the bed loading.

Finally, this method is classified as active and wake control method. This technique is an important method to control the flow separation. Moreover, this method significantly affects the stability of the boundary layer and the transition to turbulence. As an active method, typically a high source of energy is required for this method especially for underwater flows in ocean engineering applications. Beside this, base bleed, among other techniques, requires a relatively high power input because it is applied inside the recirculation region. As mentioned by researchers, the forcing

close to the separation point generally has the foremost control efficiency. Hence, it is recommended to consider this point for improving the efficiency of this method. Researchers reported a drag reduction up to 30% by synthetic jets (Feng et al. (2010)). Due to the alternative effects of unsteady blowing and suction, synthetic jets have good efficiency in delaying separation and reducing the drag coefficient. The mass-flux produced by these techniques is an important point that affects the energy consumption by these methods. The effect of the mass-flux requires further studies.

Table 4 summarizes the researches on application of secondary flows to control the vortex shedding and flow separation of a bluff body. As presented in this table, most of these researches cover low Reynolds number regimes. The future researches should be focused on the critical or supercritical Reynolds numbers.

2.1.4. Control of vortex shedding by a magnetic field (MHD)

This method is classified as active and boundary layer control method. Magnetohydrodynamics (MHD) is the physical-mathematical framework that is concerned with the dynamics of magnetic fields in electrically conducting fluids. Any movement of a conducting fluid in a magnetic field, B, generates electric currents, j. Each unit volume of liquid having j and B experiences a resistive type force, known as the Lorentz force. This force can be calculated by, see e.g. Rashidi et al. (2015b) and Valipour et al. (2014a):

$$F_{\text{Lorentz force}} = \sigma(V \times B \times B) \tag{3}$$

where V, B and σ are the fluid velocity vector, uniform magnetic field strength vector and electrical conductivity of the fluid, respectively. This force acts on the downstream flow in opposite of the flow direction and reduces the flow velocity, leading to flow stabilization. This method is shown to be effective in controlling the flows over tubular heat exchangers, pipelines, suspension wires, and suspension bridges. Fig. 8 shows the electrodes and permanent magnets to generate Lorentz force to control the separated flows around a hydrofoil. Fig. 9 shows the effects of an external magnetic field in horizontal direction (streamwise magnetic field) on vorticity contours. As shown in this figure, the flow stabilizes and changes its distribution from the time-dependent behavior with vortex shedding to the steady state with a symmetric shape along the centerline for strong magnetic field. It should be noted that if the magnetic field is used in the horizontal direction, the vertical force acts in the negative y-direction and this leads to retard the motion of the fluid (See Eq. 3).

Mutschke et al. (1998) studied the problem of controlling wake behind a circular cylinder by utilizing magnetic fields in liquid metal flows. They performed a numerical simulation on the unsteady two-dimensional flow. Weier and Gerbeth (2004) experimentally investigated the application of time periodic Lorentz forces in controlling the suction side flow on a NACA 0015 hydrofoil for the low Reynolds number range of $10^4 < \text{Re} < 10^5$. It was found that the Lorentz force allows for a great flexibility to provide the time dependency of the forcing. Chen and Aubry (2005) numerically developed an active control algorithm for manipulating wake flows past a two-dimensional circular obstacle. They used control actuators in their algorithm, where the actuators exert Lorentz forces over the entire surface of the obstacle. Their results showed that vortex shedding may completely disappear and the total drag coefficient would decrease as the Lorentz force increases for $N > 3$, where N is the interaction parameter, defined as the ratio of the electromagnetic force to the inertial force. This was found to be due to the predominant role played by the pressure on the total drag coefficient.

Control of vortex shedding from a bluff body using imposed magnetic field was studied numerically by Singha et al. (2007). A

Table 4
Researches on application of generating a secondary flow (suction, blowing, bleed and synthetic jets) to control the vortex shedding and flow separation of a bluff body.

Authors	Type of research	Type of fluid	Reynolds number	Spatial dimensions	Type of bluff body	Type of injection
Seal and Smith (1999)	Experimental	Water	1.09×10^4	–	Circular	Suction insert at a streamwise location 90 cm from the leading edge of cylinder
Delaunay and Kaiktsis (2001)	Numerical	–	1–90	2D	Circular	Suction and blowing applied at the cylinder base
Tensi et al. (2002)	Experimental	Air	1.0×10^5	–	Circular	Synthetic jet at the wall of the cylinder
Li et al. (2003)	Numerical	–	Less than 1.1×10^2	2D	Circular	Injection and suction at the surface of the cylinder
Layek et al. (2008)	Numerical	–	6.0×10^2	2D	Square	Uniform suction and blowing at channel walls
Feng and Wang (2010)	Experimental	Water	9.5×10^2	–	Circular	Synthetic jet at the rear stagnation point
Feng et al. (2010)	Experimental	Water	9.5×10^2 and 1.6×10^3	–	Circular	Synthetic jet at the rear stagnation point
Feng et al. (2011)	Experimental	Water	9.5×10^2 and 1.8×10^3	–	Circular	Synthetic jet at the back stagnation point
Chen et al. (2013)	Experimental	Air	Unknown	–	Circular	Suction from lowest positions of the cylinder
Joseph et al. (2013)	Experimental	Air	1.1×10^6–2.8×10^6	–	Ahmed body	Micro-jets
Muralidharan et al. (2013)	Numerical	–	1.0×10^2 and 3.9×10^3	2D	Circular	Suction and blowing from the cylinder surface
Chaligné et al. (2014)	Experimental	Air	1.76×10^5	–	Square	Pulsed jets at upper edge of the cylinder
Liu and Feng (2015)	Numerical	–	5.0×10^2	2D	Circular	Two synthetic jet at the mean separation points
Sohankar et al. (2015)	Numerical	–	70–1.5×10^2	2D	Square	Uniform suction and blowing from the cylinder surface

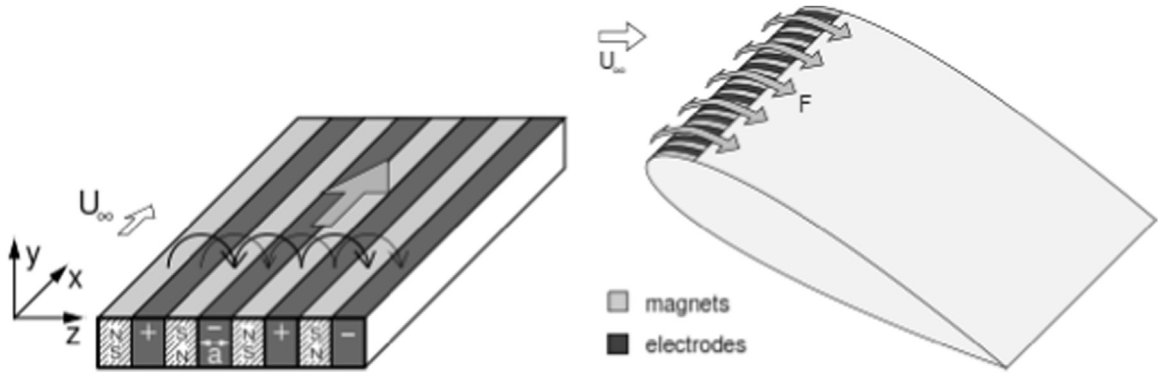

Fig. 8. Electrodes and permanent magnets to generate Lorentz force to control the separated flows around a hydrofoil (Figure reprinted from Weier and Gerbeth (2004) with permission from the publisher).

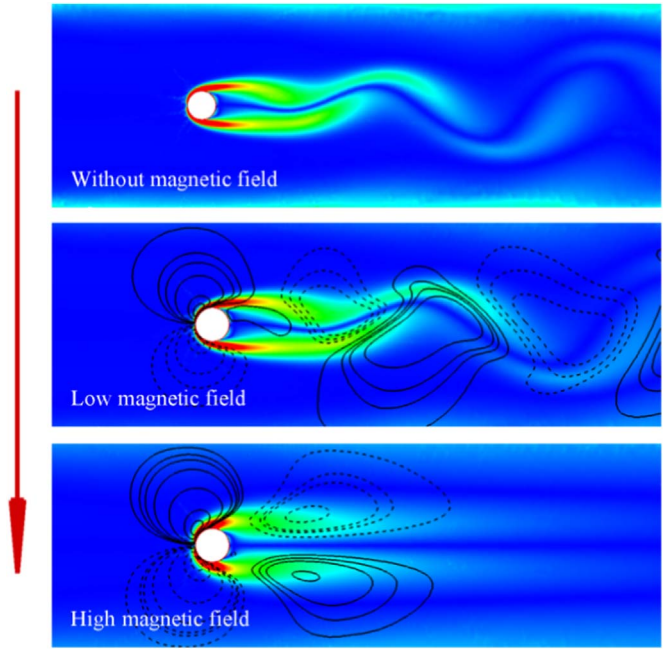

Fig. 9. Contours of vorticity at different magnetic field strength at Re = 100 (Flow is from left to right).

2-D incompressible laminar viscous flow past a square obstacle placed inside the channel was considered. This study showed that the periodic vortex shedding can be completely eliminated by applying a strong magnetic field. Singha and Sinhamahapatra (2011) numerically investigated effects of an imposed transverse magnetic field on control of vortex shedding from a circular cylinder for Reynolds numbers varying from 50 to 250. They observed that the separated zone behind the obstacle in a steady flow decreases with increase in the magnetic field strength. Chatterjee et al. (2012) controlled flow separation around 2-D bluff bodies by exerting a transverse magnetic field. The computations were performed for low Reynolds numbers in the range of 10-40, and two-dimensional circular and square cross sections. It was found that length of the wake region and separation angle decrease with the increase in the magnetic field strength.

Zhang et al. (2014) presented a suppression mechanism for vortex-induced vibration by symmetric Lorentz forces. They used a 2-D moving circular cylinder and numerically studied the effects of Lorentz force for controlling the vortex-induced vibration (VIV) of a circular cylinder at Re = 150. They concluded that the applied Lorentz force affects the phase angles among the obstacle displacement, the total lift force and the vortex induced lift force. Rashidi et al. (2015c) controlled the wake structure behind a square obstacle in channel flow by exerting a horizontal magnetic field. They defined two parameters for controlling the flow: critical Stuart number, defined as the Stuart number where unsteady flow becomes steady; and disappearance Stuart number, defined to measure the strength of the inserted magnetic field required for disappearing the recirculating wake. They observed that critical and disappearance Stuart numbers increase for higher Reynolds numbers. Bovand et al. (2015c) repeated this problem for a porous circular obstacle and they used a cross-radial magnetic field to control the flow. They found that the value of critical Stuart number for suppressing the vortex shedding decreases when Darcy number increases. Also, the disappearance Stuart number decreases with increase in Darcy numbers.

Rashidi and Esfahani (2015e) controlled instabilities of heat transfer from an obstacle in a channel by a horizontal magnetic field, and showed that existence of channel wall decreases the effects of Stuart number on heat transfer compared with corresponding infinite-domain case. Also, they found that unsteadiness in temperature field increases with increase in Reynolds number. Therefore, a stronger magnetic field is needed to control the instabilities of heat transfer at higher Reynolds number.

Finally, this method is classified as an active boundary layer control method. This method is required an electrically conducting fluid (i.e. seawater) as working fluid. Therefore, this method is very practical in ocean engineering applications. A resistive force (Lorentz force) is created by applying a magnetic field in a moving fluid. This force tends to retard the motion of the fluid and can be used as a damping force to supress the vortex shedding from a bluff body. The magnetic field can vary in space and time and therefore, it can create a flexible force, which can be adjusted to achieve a specific purpose. No mechanically moving parts are necessary to persuade this changeable force, so there is no reason for additional attrition. As discussed in literature, the drag force can be decreased by a suitable selection of Lorentz force distribution that can be used in marine vehicles, see e.g. Bovand et al. (2015c).

Table 5 summarizes the researches on application of MHD to control the vortex shedding and flow separation of a bluff body. As shown in this table, the ranges of Reynolds numbers are very low. Such low values of Reynolds number are only practical for some liquid metal flows in nuclear or semi-conductor applications and microfluidic applications. Therefore, more studies are required to cover the critical and transcritical Reynolds numbers (i.e. larger than 1.0×10^5). Moreover, most of researches performed using this method, are numerical. Further experimental studies are necessary on this method. Moreover, the Lorentz force acts as a volume force on entire the domain. It would be interesting to have a tunable force to act only in specific regions of the flow. This

Table 5
Researches on application of MHD to control the vortex shedding and flow separation of a bluff body.

Authors	Type of research	Type of fluid	Reynolds number	Spatial dimensions
Mutschke et al. (1998)	Numerical	–	$50-3.0\times10^2$	2D/3D
Weier et al. (1998)	Experimental/Numerical	Solution of 10% copper sulfate ($CuSO_4$) and 5% sulphuricacid (H_2SO)	2.0×10^2	2D/3D
Posdziech and Grundmann (2001)	Numerical	–	$10-3.0\times10^2$	2D
Weier and Gerbeth (2004)	Experimental	Electrolyte (NaOH solution)	$5.2\times10^4-1.5\times10^5$	–
Chen and Aubry (2005)	Numerical	–	2.0×10^2	2D
Mutschke et al. (2006)	Numerical	–	5.0×10^2 and 6.0×10^2	2D
Singha et al. (2007)	Numerical	–	$50-2.5\times10^2$	2D (Square cylinder)
Singha and Sinhamahapatra (2011)	Numerical	–	$50-2.5\times10^2$	2D (Circular cylinder)
Chatterjee et al. (2012)	Numerical	–	$10-40$	2D
Zhang et al. (2014)	Numerical	–	1.5×10^2	2D
Bovand et al. (2015c)	Numerical	–	$1–2.0\times10^2$	2D
Rashidi et al. (2015c)	Numerical	–	$1–2.5\times10^2$	2D

supposition can be used in future researches on applications of this method in flow control.

2.1.5. *Control of vortex shedding by rotary oscillations or rotary non-oscillations*

This method is classified as active and boundary layer control method. A positive or negative lift can be created by rotating a cylinder. The rotation in this method can be both oscillating or non-oscillating. Note that constant rotation results in no oscillations. The direction of lift depends on the direction of the spin. This force can lead to a complete vortex shedding behind the obstacle. In this method, the near-wake structure is significantly modified by the interaction between the rotationally oscillating surface and the surrounding fluid. It is worth mentioning that the oscillation of an obstacle leads to weaken the wake and transfers the formation region closer behind the obstacle. This interaction leads to acceleration or deceleration of the fluid flow around the obstacle according to the direction of rotation. This method is widely used to control the flow of tube heat exchangers, shafts, drilling of oil wells, nuclear reactor fuel rods and steel suspension bridge cables. Fig. 10 shows an experimental setup to control the wake behind a circular cylinder by rotary oscillations. Fig. 11 shows the streamlines and vorticity at different rotational speeds at $Re=1.0\times10^2$. As shown in this figure, a complete suppression of flow unsteadiness can be achieved with an increase in rotation rate. In this figure, α is the dimensionless rotation rate given by:

$$\alpha = \frac{D\omega}{2U} \tag{4}$$

where ω, U, and D are the rotational speed of cylinder, free flow velocity and cylinder diameter, respectively.

Baek and Sung (1998) performed a numerical study on the flow behind a rotary oscillating circular obstacle at $Re=1.1\times10^2$. They found that the counterclockwise rotation leads to large-scale vortex move downward. Sengupta et al. (2007) controlled the flow for a 2D circular obstacle executing rotary oscillation using genetic algorithm at $Re=1.5\times10^4$. The 2D Navier–Stokes equations are solved numerically by using a fast viscous-vortex method. They calculated the maximum rotation rate and the forcing frequency of the rotary oscillation for the purpose of drag reduction. Lee and Lee (2008) presented experimentally the PIV measurements of the wake behind a rotationally oscillating circular obstacle at $Re=4.14\times10^3$. They observed that the length of the vortex formation region decreases with increase in the forcing frequency when the frequency ratio is smaller than 1.0. Also, they showed that the rotational oscillatory motion of a circular obstacle is an effective and promising technique for controlling the near-wake flow structure. The method is used by others, e.g., Korkischko and Meneghini (2012), Chan et al. (2011) investigated numerically and experimentally the vortex suppression and drag reduction around a pair of counter-rotating circular cylinders for $Re=1.0\times10^2$–2.0×10^2. They observed that the unsteady wake can be suppressed by creating a rotation for each cylinder in the opposite direction. They claimed that the drag force can be reduced to zero for a higher rotational speeds. Flinois and Colonius (2015) suppressed the vortex shedding of a circular cylinder using body rotation. They were able to reduce the drag by about 19% and effectively suppressed the vortex shedding.

Finally, this method is classified as an active boundary layer control method. The oscillation of an obstacle leads to weakening the wake and transfers the formation region closer behind the obstacle. Moreover, the interaction between the rotationally oscillating cylinder and the surrounding fluid leads to modification of the near-wake structure substantially by accelerating or decelerating the flow near the cylinder, depending on the rotation direction. The drag force may be reduced up to 80% at a high forcing frequency. Since the rotation rates can be adjusted by a simple electronic device and mechanical means, this control method is

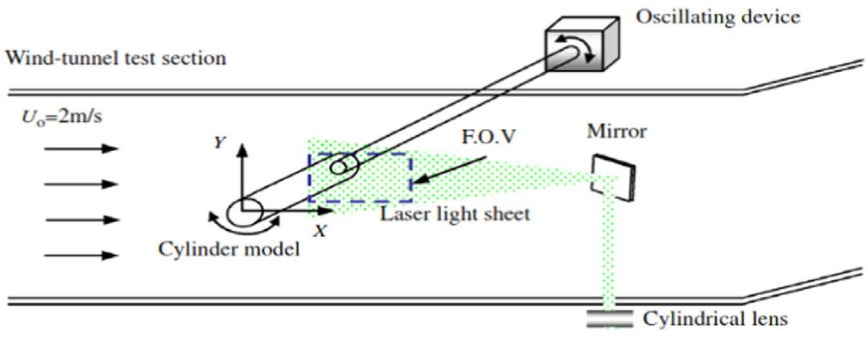

Fig. 10. An experimental setup to control the wake behind a circular cylinder by rotary oscillations (Figure reprinted from Lee and Lee (2008) with permission from the publisher).

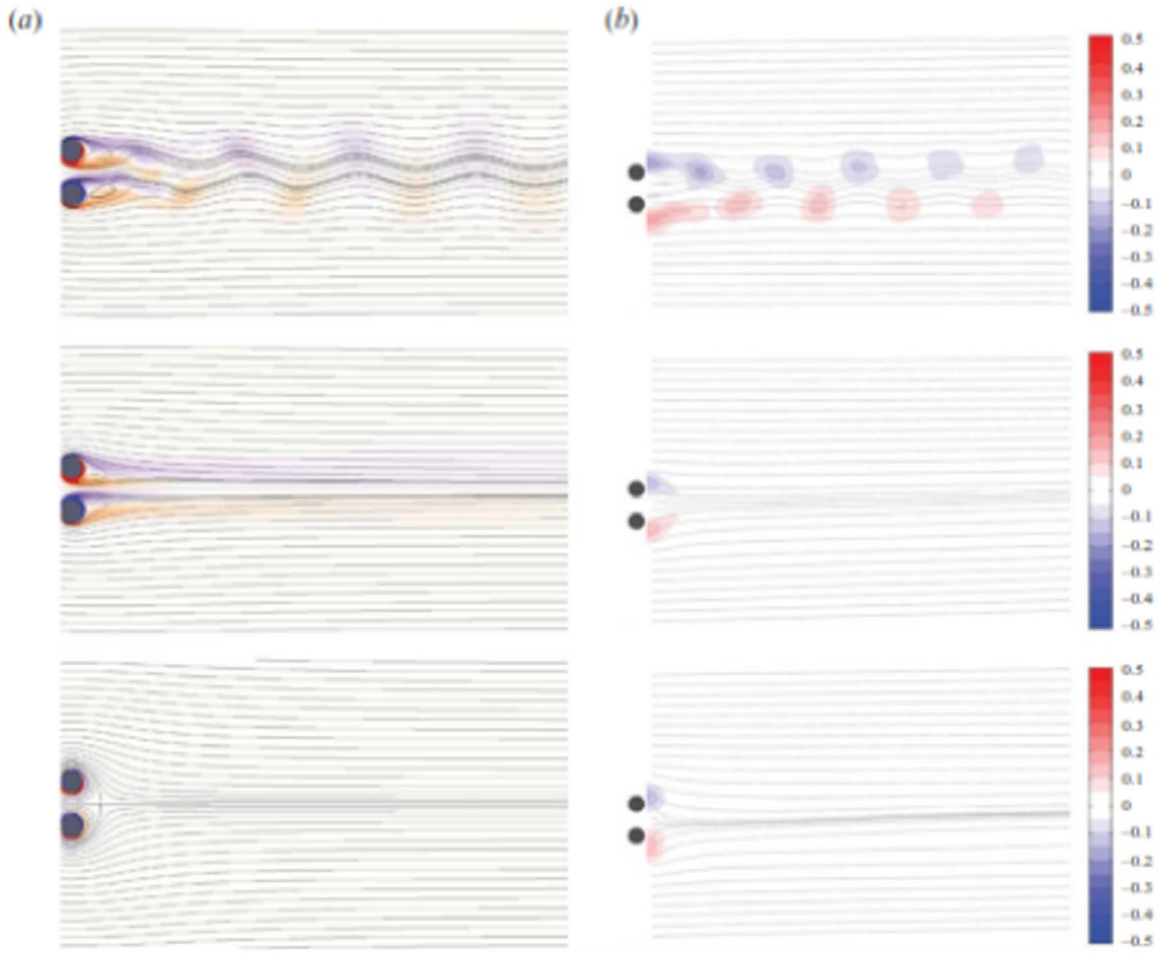

Fig. 11. Configuration of streamlines and vorticity at different rotational speedsRe=100 a) Computational results; b) Experimental results. First row, α=1.2; second row, α=1.5; third row α=3 (Flow is from left to right; Figure reprinted from Chan et al. (2011) with permission from the publisher).

suitable for practical applications. This method can be used to control the near-wake flow structure.

Table 6 summarizes researches on the application of rotary oscillations to control the vortex shedding and flow separation of a bluff body. A comparison between different directions of oscillating, i.e. in-line or transverse linear oscillations, would be interesting for future researches. In addition, there are some other types of oscillation such as flow perturbations and imposed sound field that can be used as a flow control method. Although, there is a few research about these, e.g. Armstrong et al. (1986) and Blevins (1985), but there is need for further studies as these types are more applicable in ocean engineering.

2.1.6. *Control of vortex shedding by thermal effects*

This method is classified as active and boundary layer control method. Buoyancy effects around a bluff body appear in the near wake when the level of heating is high. Buoyancy effect creates inertia and viscous forces around the obstacle and this results in to delay in flow separation and suppression of the vortex shedding. Increase of the heat input in the obstacle leads to a suppression of the vortex shedding for air flow while for the liquid flowing around a heated obstacle this effect is inverse. This opposite behavior for gases and liquids suggest that this control is due to both changes of dynamic viscosity and density with temperature. The changes of the viscosity and the density lead to slight changes in velocity profiles and consequently amplitude of the shed vortices and instability conditions. The thermal buoyancy is a natural way to control the boundary layer separation over a cylinder. Therefore, it can be used in many engineering applications. Fig. 12 shows the application of thermocouple to measure the temperature gradient on the surface of the cylinder for controlling the flow.

Fig. 13 shows the contours of streamlines around a square obstacle for different Richardson numbers is defined as $Ri=Gr/Re^2$, where $Gr = g\beta(T_w - T_\infty)D^3/\nu^2$ and g, β, T_∞, T_w and ν are the

Table 6
Researches on application of rotary oscillations to control the vortex shedding and flow separation of a bluff body.

Authors	Type of research	Type of fluid	Reynolds number	Spatial dimensions	Type of rotation
Tokumaru and Diimotakis (1989)	Experimental	water	1.5×10^4	–	Oscillating
Baek and Sung (1998)	Numerical	–	1.1×10^2	2D	Oscillating
Sengupta et al. (2007)	Numerical	–	1.5×10^4	2D	Oscillating
S.J. Lee and J.Y. Lee (2006)	Experimental	Air	4.14×10^3	–	Oscillating
Chan et al. (2011)	Experimental/Numerical	water	1.0×10^2–2.0×10^2	2D for numerical part	Non-oscillating
Flinois and Colonius (2015)	Numerical	–	75–200	2D	Oscillating/ Non-oscillating

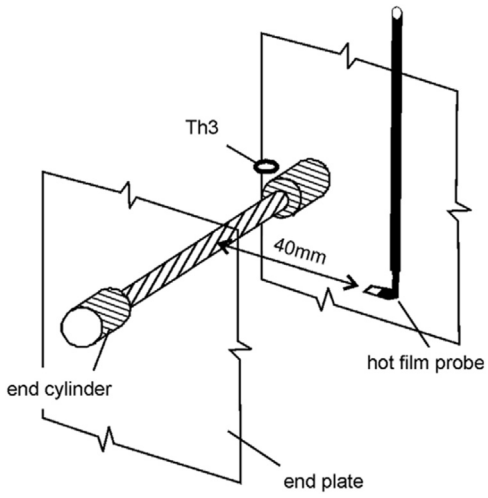

Fig. 12. Application of thermocouple to measure the temperature gradient on the surface of the cylinder for controlling the flow (Figure reprinted from Vit et al. (2007) with permission from the publisher).

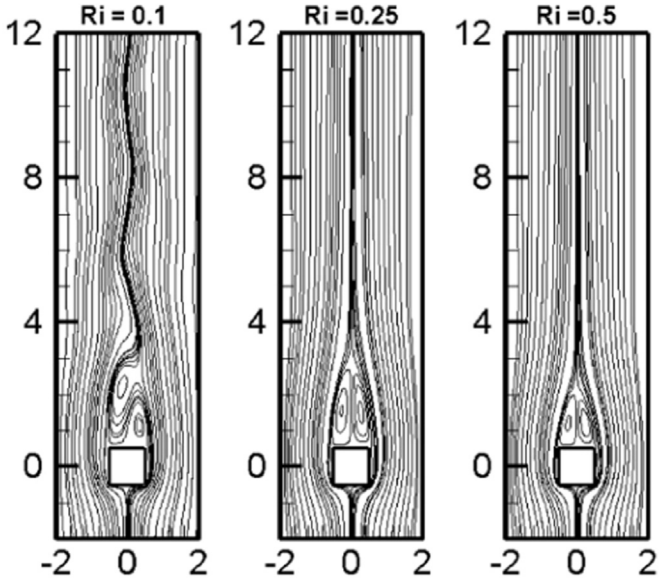

Fig. 13. Contours of streamlines around square obstacle for different Richardson numbers (Ri) at a constant Reynolds number,$Re = 1.0 \times 10^2$ (Flow is from down to up; Figure reprinted from Chatterjee (2014) with permission from the publisher).

gravitational acceleration, volumetric expansion coefficient, free stream temperature, cylinder temperature and kinematic viscosity of fluid, respectively. As the buoyancy effect increases, Ri becomes larger. In this method, location of separation point changes due to the increase of fluid dynamic viscosity. As shown in Fig. 13, as Ri increases, and for a constant Re, the flow stabilizes and changes distribution from a time-dependent flow with vortex shedding to steady state flow with a symmetric shape along the centerline. In this figure, spatial coordinates in the horizontal and vertical directions are dimensionless.

This method was used by Lecordier et al. (1991) in an experimental study on control of vortex shedding behind circular cylinders at low Reynolds numbers by heating the cylinder. They found that the thermal effect method can lead to a complete suppression of periodic oscillations in the wake region for $90 < Re < 1.2 \times 10^2$. Later, Lecordier et al. (2000) experimentally controlled the formation of vortex shedding behind two 2-D bluff bodies (circular cylinder and a flat ribbon) by thermal effect at low Reynolds numbers. It was found that the method mainly depends on the type of the fluid. They showed that a suppression of vortex shedding occurs with increase in the heat input to the cylinder or ribbon for air flow, however, an opposite effect was observed in a water flowing around a heated cylinder or ribbon. Therefore, both cooling and heating can be used in this method.

In a numerical study, Chatterjee (2014) investigated the dual role of thermal effects for controlling boundary layer separation around cylinders. Circular and square shaped cylinders were considered in this research. They observed that the thermal buoyancy can change the flow from time-dependent pattern with vortex shedding in the wake to steady re-circulatory flow with complete suppression of vortex shedding. Also, the steady flow may turn into an unsteady periodic flow with initiation of vortex shedding by the action of thermal buoyancy when the buoyancy acts in a cross wise direction to the incoming flow. Therefore, the buoyancy has positive or negative effects on the flow control. It acts as a destabilizer when acting perpendicular to the flow direction. They showed that the minimum heating that is needed to suppress the vortex shedding increases with increase in Reynolds number. Moreover, they observed that a square obstacle requires more heating to suppress the vortex shedding in comparison to the circular one.

Chatterjee and Mondal (2014) numerically controlled the flow separation around bluff obstacles by superimposing thermal buoyancy. Results show that, for lower Prandtl number, higher heating is required for a complete suppression of flow separation around the bluff bodies. Circular and square cross-sections were used, and it was found that the square obstacle requires more heating when compared with the corresponding circular obstacle for complete suppression of flow separation. Chatterjee and Ray (2014) repeated the study for a triangular obstacle, and found that the wake length decreases with increasing strength of buoyancy and it completely vanishes with further increase in strength of buoyancy.

Finally, this method is classified as active boundary layer control method. According to this method, the density and viscosity of the fluid are changed due heating the fluid. This leads to creation of buoyancy forces and slight changes in velocity profiles in near wake and consequently instability of the shedding vortices. We considered this method in active classifications, however thermal buoyancy can be inherently a natural way to control the flow. Note that the thermal buoyancy can have a dual role. It stabilizes the flow when acting along the flow direction and conversely it destabilizes the flow when acting perpendicular to the flow direction. As shown by researchers, e.g. Chatterjee and Ray (2014), the change in the fluid type has considerable effects on the suppression behavior in this method. More heating is required to completely suppress the flow separation around the bluff bodies for the fluids with low values of Prandtl number. Therefore, this method is more suitable for water rather than air from the viewpoint of energy consumption.

Table 7 summarizes researches about application of thermal effects to control the vortex shedding and flow separation of a bluff body. As shown in this table, these researches covered very low Reynolds number and two-dimensional objects. As a result, the ability of this method to suppress the vortex shedding for moderate and high Reynolds numbers is questionable and more research is necessary to answer this question. Note that the flow separation is controlled at lower values of Reynolds number (i.e. $Re < 40$) while, the vortex shedding is suppressed for larger Reynolds number ($50 < Re < 1.5 \times 10^2$). None of these researches (except the paper of Chatterjee and Sinha (2014)) focused on the effects of heating on aerodynamic or hydrodynamic forces such as drag and lift forces. Therefore, further studies are necessary for these forces.

Table 7
Researches on application of thermal effects to control the vortex shedding and flow separation of a bluff body.

Authors	Type of research	Type of fluid	Reynolds number	Spatial dimensions
Lecordier et al. (1991)	Experimental	Air	$45-1.2\times10^2$	–
Lecordier et al. (2000)	Experimental	Air and water	34–75	–
Chatterjee (2014)	Numerical	Air	$10-1.5\times10^2$	2D
Chatterjee and Mondal (2014)	Numerical	Air and water	10–40	2D
Chatterjee and Ray (2014)	Numerical	Pr=50(Pr denotes the Prandtl number)	5–30	2D
Chatterjee and Sinha (2014)	Numerical	Air	5–45	2D

2.1.7. Control of vortex shedding by other active methods

Huang (1995) experimentally suppressed the vortex shedding from a circular obstacle by internal acoustic excitation for Reynolds numbers in a range of $Re=4\times10^3$ to $Re=8.0\times10^3$. Their results showed that the vortex shedding peak decreases noticeably only in a very narrow excitation range. The optimal sound level is located at this range. Bimbato et al. (2013) numerically controlled vortex shedding on a 2-D circular obstacle by using a moving ground plane for $Re=1.0\times10^5$. Obstacle is placed near this ground plane. Their results showed that when a circular obstacle is placed closer to the ground, the vortex shedding suppresses by Venturi effect, and drag force decreases due to this suppression.

2.2. Passive control methods

2.2.1. Control of vortex shedding by surface roughness

Surface roughness is classified as passive and boundary layer control method. Surface roughness affects the location of boundary layer separation point and consequently the unsteady and steady force around the obstacle. These effects are created in boundary layer by two approaches. The transition moves forward on the surface of obstacle due to the roughness on the surface; and the roughness makes the velocity profile less full in beneath the turbulent boundary layer, see e.g. Shih et al. (1993). This method has been typically used as a passive control approach, and is utilize in offshore and marine application, such as platform pillars, pipelines and risers, see e.g. Zhou et al. (2015). Fig. 14 shows two rough cylinders that were used in the experiments conducted by Zhou et al. (2015) to control the flow. Chang et al. (2011) performed an experimental passive turbulence control (PTC) by surface roughness for a circular obstacle in a steady flow at $3.0\times10^4<Re<1.2\times10^5$. They showed that for a smooth obstacle about seven vortices shed per cycle, but it decreased to about five vortices per cycle for a rough obstacle. Kiu et al. (2011) investigated the effects of uniform surface roughness on vortex-induced vibration of towed vertical cylinders. They found that the rough obstacles have a higher Strouhal number than a smooth obstacle. Gao et al. (2015) experimentally studied the effects of surface roughness on the vortex-induced vibration response of a flexible obstacle. They observed that the displacement response decreases and the vortex-shedding frequency increases with increase in surface roughness. Also, rough obstacles have a narrower lock-in region than a smooth obstacle. In another study, Zhou et al. (2015) experimentally investigated the force and flow characteristics of a circular obstacle with uniform surface roughness at $6.0\times10^3<Re<8.0\times10^4$. They found that the mean drag coefficient on the cylinder and the root-mean-square of lift coefficient decrease with increase in surface roughness.

Finally, this method is classified as passive boundary layer control method. As mentioned in the literatures, surface roughness leads to delay in boundary layer separation. Moreover, there is a faster transition from laminar to turbulent regime for a bluff body with rough surfaces. This leads to an abrupt reduction in the drag coefficient, see e.g. Achenbach (1971). Therefore, this method is suitable for subcritical Reynolds numbers. This method has a more practical application due to its easier manufacturing, simpler installation and lower costs. The marine organisms grow on the surface of the marine structures over a period of time. This leads to increase in the surface roughness of the structure. As a result, it is important to study the effects of surface roughness.

Gao et al. (2015) summarized the recent researches on the application of the surface roughness to control the vortex shedding behind a bluff body. The results of these researches are presented in Table 8. The ranges of Reynolds number, aspect ratio,

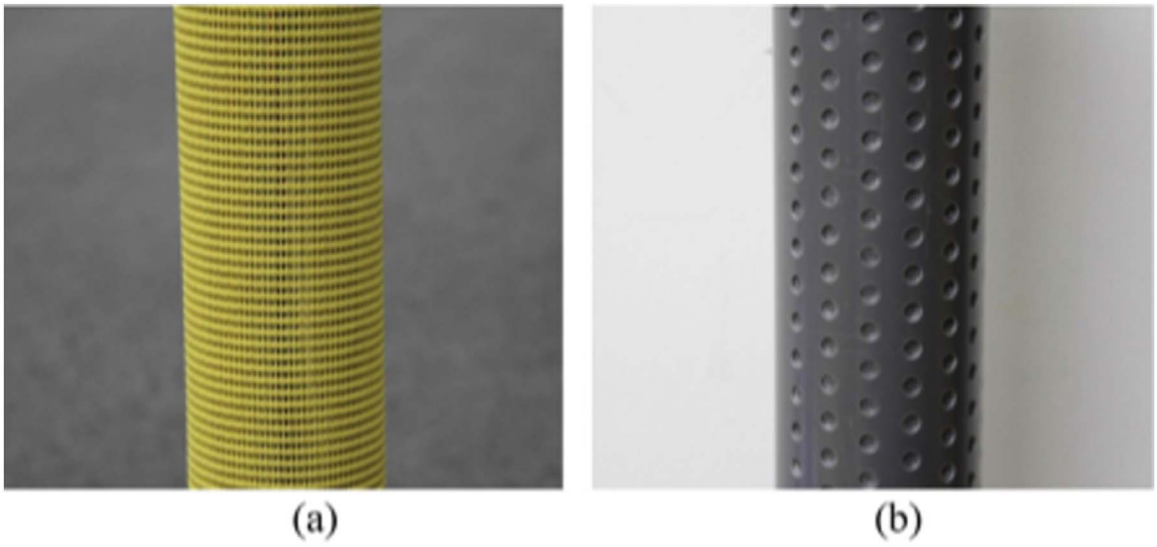

Fig. 14. The rough circular cylinders with (a) netting and (b) dimples. (Figure reprinted from Zhou et al. (2015) with permission from the publisher).

Table 8
Previous studies on the surface roughness controls for flow over a cylinder (Table reprinted from Geo et al. (2015) with permission from the publisher).

Authors	Type of research	Aspect ratio (Cylinder length/Cylinder diameter)	Cylinder conditions	Reynolds number	Surface roughness (equivalent roughness height/ Cylinder diameter)	Type of roughness
Air						
Achenbach (1971)	Experimental	3.33	Stationary	4.0×10^{4}–3.0×10^{6}	1.1×10^{-3}–9.0×10^{-3}	Sand roughness
Achenbach and Heinecke (1981)	Experimental	3.38	Stationary	6.0×10^{3}–5.0×10^{6}	7.5×10^{-4}–3.0×10^{-2}	Pyramidal roughness
Nakamura and Tomonari (1982)	Experimental	3.33	Stationary	$4.0\times10^{4}-1.7\times10^{6}$	$9.0\times10^{-4}-1.0\times10^{-2}$	Roughness strips
Ribeiro (1991a, 1991b)	Experimental	6.1	Stationary	$5.0\times10^{4}-4.0\times10^{5}$	$1.8\times10^{-3}-1.2\times10^{-2}$	Sand paper, wire screen and nylon ribs
Bearman and Harvey (1993)	Experimental	12.26	Stationary	$2.0\times10^{4}-3.0\times10^{5}$	$4.5\times10^{-3}-9.0\times10^{-3}$	Dimpled surface
Shih et al. (1993)	Experimental	8	Stationary	$1.0\times10^{5}-1.0\times10^{7}$	$3\times10^{-4}-1.01\times10^{-2}$	Screens
Okajima et al. (1999)	Experimental	1.83	Oscillating	$2.5\times10^{4}-3.2\times10^{5}$	$5.0\times10^{-3}-3.8\times10^{-8}$	Spherical glass bead particles or 64 stranded cables with 6 mm diameter that are attached to the cylinder surface
Water						
Allen and Henning (2001)	Experimental	84.6	Oscillating	$1.8\times10^{5}-6.5\times10^{5}$	$5.1\times10^{-5}-5.8\times10^{-3}$	Rough pipes that consisted simply of macrospheres glued to their surface
Bernitsas et al. (2008); Bernitsas and Raghavan (2008)	Experimental	7.2–14.4	Oscillating	$8.0\times10^{3}-2.0\times10^{5}$	$1.4\times10^{-3}-4.2\times10^{-3}$	Sandpaper strips
Kiu et al. (2011)	Experimental	8.0	Oscillating	$1.7\times10^{4}-8.3\times10^{4}$	$2.8\times10^{-4}-1.4\times10^{-2}$	Sandpapers with known mean particle diameters
Chang et al. (2011)	Experimental	10.3	Oscillating	$3.0\times10^{4}-1.2\times10^{5}$	$5.4\times10^{-4}-4.68\times10^{-3}$	Roughness strips
Zhou et al. (2015)	Experimental	10	Stationary	$6.0\times10^{3}-8\times10^{4}$	$2.8\times10^{-3}-2.5\times10^{-2}$	Netting and dimples
Gao et al. (2015)	Experimental	48.32	Oscillating	$2.5\times10^{4}-1.8\times10^{5}$	$1.14\times10^{-4}-1.2\times10^{-2}$	Sand with different particle diameters

Table 9
Researches on application of permeable wall to control the vortex shedding and flow separation of a bluff body.

Authors	Type of research	Type of fluid	Reynolds number	Spatial dimensions
Ozkan et al. (2012)	Experimental	Water	8.5×10^3	–
Gozmen et al. (2013a)	Experimental	Water	5.0×10^3	–
Mimeau et al. (2014)	Numerical	–	5.5×10^2 and 3.0×10^3	2D
Rashidi et al. (2014b)	Numerical	–	1–45	2D
Valipour et al. (2014b)	Numerical	–	1–45	2D

surface roughness, and cylinder conditions for each research are presented in this table. There are very few researches on the effect of surface roughness for oscillating cylinder in wind. The VIV (vortex-induced vibration) for a bluff body is important in wind flows. These papers focused on determining the pressure distribution, flow separation, and Strouhal number characteristics. However, the aerodynamic excitation of the body is not discussed in these papers. Structural–dynamic response is important from the practical point of view. Accordingly, many questions remain unanswered in wind flows. Moreover, most of the studies on this control method are conducted experimentally, while the numerical studies in this field are very limited. Most of previous studies focused on the uniform distribution of roughness over the entire of the surface. More attention is required to study the effects of roughness distributions and local roughness. It can also be seen that this method works well at subcritical Reynolds numbers but does not work very good at a lower values of Reynolds number, see e.g. Achenbach (1971), Achenbach and Heinecke (1981).

2.2.2. Control of vortex shedding by porous and permeable walls

This method is classified as passive wake control method. Gozmen et al. (2013a) experimentally controlled the downstream flow behind a circular obstacle in deep water by using an outer permeable obstacle. They reported that the outer permeable obstacle significantly suppresses the vortex shedding behind two obstacles with increase in the porosity defined as ratio of the gap area on the region to the whole body surface area. Also, they found that porosity of 0.7 is the most suitable case to control the vortex shedding behind the obstacle. A fixed value of Reynolds number, $Re = 5.0 \times 10^3$, was considered in all experiments in this study. In another research, Mimeau et al. (2014) numerically controlled the flow around a semi-circular cylinder by using a porous layer for laminar and transitional flows. The incompressible Navier-Stokes equations were used to describe the dynamics of flow. They achieved relevant control performances by introducing porous layers only at the top and bottom of the solid body permits. Also, they observed a reduction in drag by using a thin layer with intermediate permeability in both edges of the back wall.

Ozkan et al. (2012) experimentally controlled the flow characteristics around a circular cylinder by a porous outer cylinder in shallow water. They used Particle Image Velocimetry technique and suppressed the formation of an organized vortex street by porous outer cylinder. They observed that the effect of porous outer cylinder on the characteristics of inner cylinder decreases with the increase in the porosity. Pinar et al. (2015) performed an experimental study on the flow structure around permeable circular obstacles. They used Particle Image Velocimetry technique and found that the porosity had a significant effect on the control of large-scale vortical structures downstream of the obstacle. They attenuated significantly the fluctuations and prevented the formation of Karman Vortex Street by use of permeable cylinders.

Valipour et al. (2014b) numerically controlled the flow around and through a porous obstacle with diamond cross section for $Re < 50$. They observed that the critical Reynolds numbers to onset of the re-circulating wake for a porous obstacle is larger than that of a solid obstacle for intermediate and large Darcy numbers. Also, they found that this critical Reynolds number for a square obstacle is smaller than that of the diamond obstacle. Rashidi et al. (2014b) repeated this study for a porous diamond obstacle with different apex angles at $Re < 50$. The computed results showed that the critical Reynolds number for the onset of the wake in a porous obstacle decreases with an increase in the apex angle. Note that finite volume method was used to solve the continuity and Navier–Stokes equations in above two papers.

Finally, this method is classified as a passive wake control method. The main control parameter in this method is porosity or void fraction of porous medium. Highly permeable media (higher porosity) are more efficient, as presented by researchers, see e.g. Rashidi et al. (2014b).

Table 9 summarizes researches on application of permeable wall to control the vortex shedding and flow separation of a bluff body. The existing studies need to be complemented by 3D researches to match the control trends that were observed in the 2D observations. Generally, there are limited studies on the 3D applications.

2.2.3. Control of vortex shedding by other passive methods

Bearman and Owen (1998) experimentally controlled the vortex shedding from a plate by a spanwise sinusoidal form at Reynolds numbers of about 4.0×10^4. They observed at least 30% reduction in drag for wavy plate in comparison with the equivalent straight bodies. Also, the vortex shedding is completely suppressed for specific ratios of peak-to-peak wave height to wavelength ratio. Lei et al. (2000) suppressed numerically vortex shedding behind a circular cylinder near a plane boundary by changing the gap ratios between cylinder and plate for different Reynolds numbers ranging from 80 to 1.0×10^3. They observed that the critical gap ratio for suppressing vortex shedding is identified at different Reynolds numbers. Also, the effect of the gap ratio on the vortex shedding frequency increases by an increase in Reynolds numbers. In another research, Straatman and Martinuzzi (2002) performed a numerical study on vortex shedding phenomena from a square obstacle near a wall. This research indicated that the suppression of vortex shedding could not be expressed simply by a cancellation of vorticity mechanism, because the vorticity generated at the wall. Graham and Huang (2010) presented a passive flow control device by flow visualization techniques for a 2-D bluff body. They tested two endplates on the bluff body (with and without the passive control system). It was found that the flow visualization model did not succeed in fully demonstrating the characteristics of the entire wake due to a flaw in the dye system design. Huang (2011) experimentally supressed vortex induced vibration (VIV) of a circular cylinder by using the helical grooves. Author introduced the triple-start helical grooves as an effective method to suppress the cylinder VIV response. Author observed 64% reduction in the maximum cross-flow VIV amplitude by this method for the cases considered in the study. Kunze and Brücker (2012) experimentally controlled vortex shedding behind a circular cylinder using self-adaptive hairy-flaps method for a Reynolds number range of $5.0 \times 10^3 < Re < 3.1 \times 10^4$. It was reported that the flow fluctuations are considerably decreased when compared to the reference cases without hairy-flaps. The deductions were about 42% and 35% for streamwise and transversal directions, respectively. Also, using self-adaptive hairy-flaps, length of the separation wake behind the obstacle and rms-values (Root mean square) of velocity components in horizontal

and vertical directions within the wake region were decreased. Xu et al. (2014) numerically suppressed the vortex-induced vibration of an elastically mounted 2-D cylinder by a traveling wave wall at $Re=2.0\times10^2$. They observed that a series of small scale vortices and formed inside the troughs of the wave downstream. These vortices control the flow separation from the obstacle wall, remove the oscillating wake and suppress the vortex-induced vibration of the obstacle.

2.3. Control of vortex shedding by employing an external element

2.3.1. Control of vortex shedding by employing an external element

Generally, external element method is classified as wake control method. For energy consuming, this method can be placed in both classifications active or passive).

First, active methods are reviewed. Nishiyama et al. (1991) conducted experiments to control the vortex shedding generated from three in-line elliptic cylinders in a uniform flow, with one of the cylinders undergoing forced transverse vibration. Efficiency of this method depends on the amplitude and frequency of the forced vibration, arrangement of the elliptic obstacles, location of the vibrating obstacle and Reynolds number ($Re=\frac{U_\infty C}{\nu}$, where C is major axis length of elliptic cylinder). Patnaik and Wei (2002) presented a control strategy for taming the wake turbulence behind a square obstacle. In their strategy, two circular cylinders are cast at the centers of the first and fourth quadrants of the main obstacle. These control cylinders rotate in clockwise and counter clockwise fashions, respectively. It is found that the wake turbulence suppresses significantly when the system is synchronized. Mittal (2001) utilized finite element method and controlled the flow past a 2-D circular obstacle by using small rotating cylinders for $Re=1.0\times10^2$ and $Re=1.0\times10^4$ and two values for the gap between the main cylinder and the control cylinders. The computed results showed that the overall drag coefficient and the unsteady aerodynamic forces acting on the main cylinder decrease considerably by using this method. Such reduction in the unsteady forces, results in smaller flow-induced vibrations from the body. Korkischko and Meneghini (2012) suppressed experimentally the vortex-induced vibration using moving surface boundary-layer control for the Reynolds number ranges from 1.6×10^3 to 7.5×10^3. They used two small rotating cylinders, placed in the boundary layer of the main cylinder for delaying the separation of the boundary layer. They observed that the maximum amplitude of oscillation for the cylinder decreases significantly by using this method. Reddy et al. (2013) analytically controlled the flow past a circular cylinder by use of two counter-rotating control cylinders. They identified the control cylinder position by using a Foppl vortex model and found that the vortex formation behind the cylinder can be suppressed by this method.

After review of the active type of this method, the passive ones are reviewed in the following:

This method is classified as passive and wake control method. External element with different shapes can be used to control the vortex shedding behind an obstacle, e.g., Kwon and Choi (1996); Huera-Huarte (2014) used Splitter plates, Oruc (2012) used Control elements with a streamlined shape, Lee and Kim (1997)) used helical wires, and Strykowski and Sreenivasan (1990); Wu et al. (2012); Zhu and Yao (2015) applied Control cylinders/rods. When an external element is placed in the vicinity of an obstacle, the vortex shedding characteristics, the mean structure and dynamic behavior of the wake and transport phenomena in the wake region change. Gap width between the element and the main obstacle, the shapes of main obstacle and control element and the placement of element are different parameters that influence the flow. The element can be placed at upstream or downstream of the bluff body in this method. This method is widely used in deepwater risers and free-spanning submarine pipelines, flourishing extraction of ocean oil and gas resources, see e.g. Wu et al. (2012). Fig. 15 shows control rods that are used to suppress the vortex-induced vibration of long flexible riser.

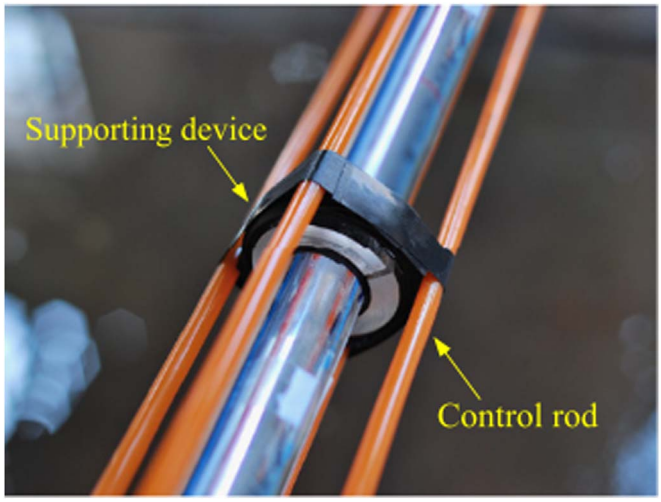

Fig. 15. Control rods that are used to suppress the vortex-induced vibration of long flexible riser (Figure reprinted from Wu et al. (2012) with permission from the publisher).

Ozkan and Akilli (2014) experimentally controlled the flow around circular obstacles by use of attached permeable plates on the obstacle wall. The plate was tilted at five different angles ($\theta=0°$, 15°, 30°, 45° and 60°), defined as the angle between the centerline of the cylinder and the plate. It was found that the maximum Reynolds shear stress (depends on the mean velocity fluctuation on two axes in turbulent flow) and turbulent kinetic energy decreased by about 72% and 66%, respectively, for the plate angles of $\theta=45°$ and 60°. Control of vortex shedding behind a circular obstacle for flows at low Reynolds numbers is performed numerically by Mittal and Raghuvanshi (2001). They used a stabilized finite element method to solve the governing equations (Navier-Stokes equations). They performed this work by using a second, much smaller, control cylinder in the near wake of the main obstacle. The computed results shown that the control obstacle provides a local favorable pressure gradient in the wake region and stabilizes the shear layer. Also, it was found that a proper placement of the control obstacle leads to a complete suppression of the vortex shedding behind the main obstacle. Maiti and Bhatt (2014) used a numerical method and suppressed the vortex shedding behind a square obstacle by utilizing a series of upstream rectangular cylinders. Their results showed that the aerodynamic forces acting downstream, decreases with an increase in the height of the upstream obstacle for a specific gap height (distance between the cylinder and wall). Bao and Tao (2013) utilized finite element formulations and controlled the wake flow behind a circular obstacle due to a laminar flow by use of parallel dual plates, attached at the trailing side of the obstacle. The stabilization of the free shear layer fluctuation and the basal cavity effect were two control mechanisms in this study. The maximum drag reduction was about 13% for $Re=1.6\times10^2$. Fig. 16 shows the configuration of streamlines (upper) and pressure contours (lower) that are presented by Bao and Tao (2013) for (a) attached dual plates control, (b) detached dual plates control, and (c) detached dual cylinders control. Shown in this figure, such mechanism is not applicable for the detached control devices because the reverse flow can cross the gap between the cylinder and device without any disturbance. This flow is driven by the adverse pressure gradient, see Fig. 16(b) and (c). Moreover, the modifications of the shear layer by these devices are presented in Fig. 17. It should be noted that the

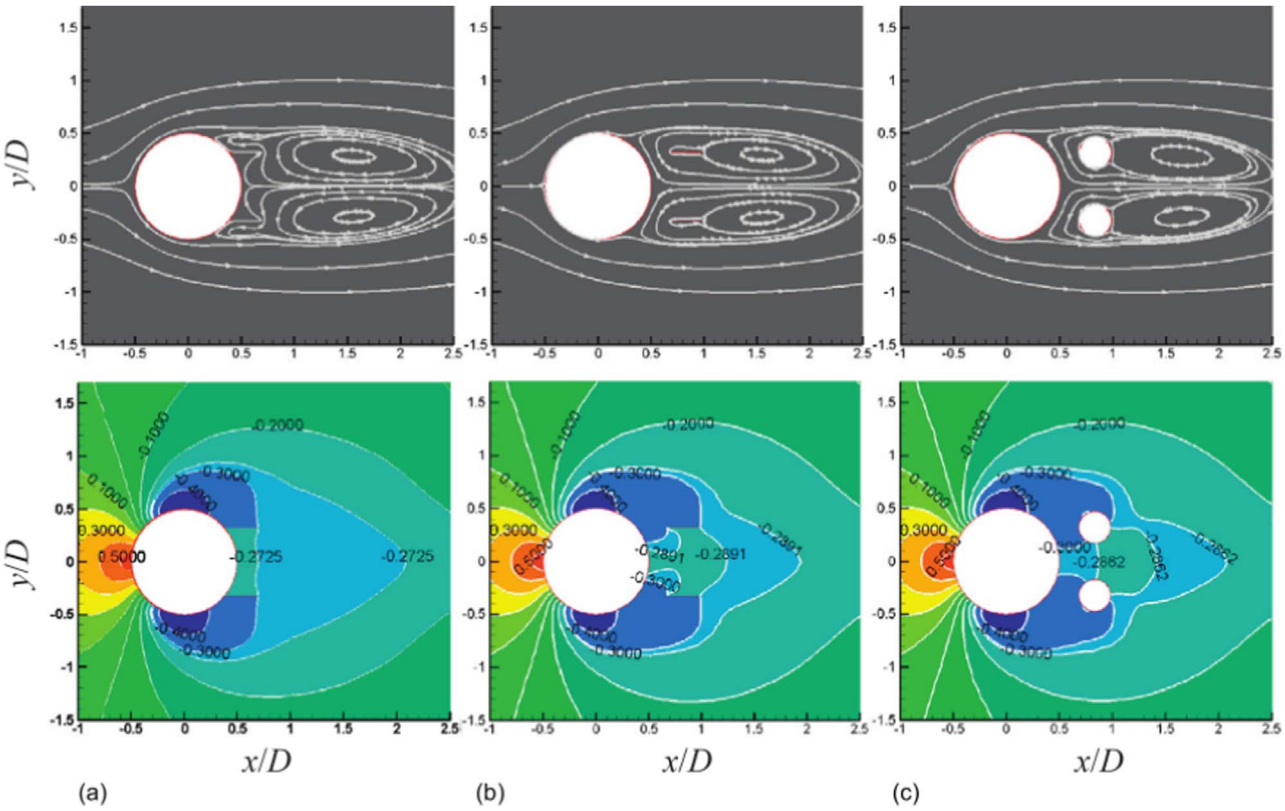

Fig. 16. Configuration of streamlines (upper) and pressure contours (lower) for (a) Attached dual plates control; (b) Detached dual plates control; (c) Detached dual cylinders control at $Re=1.0\times10^2$ (Flow is from left to right; Figure reprinted from Bao and Tao (2013) with permission from the publisher).

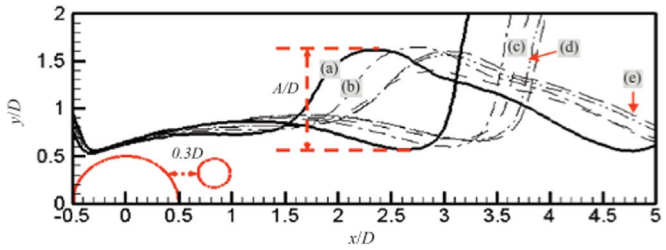

Fig. 17. The isocontour of streamwise velocity $U=U_\infty$ for cylinders with and without control devices at $Re=100$: (a) plain cylinder; (b) splitter plate control; (c) attached dual plates control; (d) detached dual plates control; and (e) dual cylinders control (Flow is from left to right; Figure reprinted from Bao and Tao (2013) with permission from the publisher).

solid and dash-dot lines in this figure refer to two time instants at which the lift force achieves its maximum and minimum, respectively. In this figure, A/D is the dimensionless fluctuation amplitude. It can be seen that the separated shear layer for the plain cylinder has the maximum fluctuation with the largest value of A/D, immediately followed by the value for the single splitter plate. This shows that the traditional splitter plate has a negligible effect on the stabilization of the fluctuation. As a result, the attached dual plates control is the most effective approach to suppress the shear layer fluctuations with the minimum amplitude. Moreover, the detached flat plate and circular cylinder devices have considerable stabilizing influences with moderate fluctuation amplitude.

Akilli et al. (2005) experimentally suppressed the vortex shedding of circular obstacle in shallow water by a splitter plate at $Re=5.0\times10^3$. Their results showed that the splitter plate has a considerable effect on the suppression of the vortex shedding for the gap ratio between 0 and 1.75D (where D is the diameter of the cylinder). The gap is defined between the base of the obstacle and the leading edge of the splitter plate. It was found that among different shapes of elements, the splitter plate was one of the most successful external devices to control the vortex shedding behind an obstacle. Chen and Shao (2013) suppressed the vortex shedding from a rectangular cylinder at low Reynolds numbers by using four kinds of elements: circular, regular triangular, square and rectangular. They performed a comparison on the application of different objects on the suppression of vortex shedding from a main cylinder at $Re=1.1\times10^2$. The mechanism of the suppression is considered from the viewpoints of stress distribution and velocity profile stability. Their study indicated that the triangular element has the smallest effective zone, whereas the square element presents the largest. The effective zone is defined as a certain location of element which vortex shedding can be suppressed and the drag and lift fluctuations can be greatly decreased.

Miau et al. (1993) experimentally suppressed low-frequency variations in vortex shedding behind a trapezoidal obstacle by a splitter plate for the Reynolds numbers in a range of 5.0×10^3 to 4.5×10^4. They found that the degree of 2-D vortex shedding is improved with suppression of low-frequency variations. Kuo and Chen (2009) numerically controlled the wake flow by two small control cylinders at $Re=80$. The computed results show that the symmetric standing eddies at downstream of the main obstacle and the delay of the vortex shedding lead to a 70–80% deduction of the fluctuating lift on the main obstacle. Vilaplana et al. (2013) experimentally controlled the turbulent wake behind a sphere by a small sphere at $Re=3.3\times10^4$. They reported that the vortex loops shed from only one side of the sphere for the reference case (without the control sphere) but the vortex loops shed closer to the symmetry axis for the control sphere placed at the center of the wake. Wu et al. (2012) experimentally suppressed the vortex-induced vibration of long flexible riser by multiple control rods for the Reynolds numbers ranging from $Re=2.4\times10^3$ to $Re=7.6\times10^3$. They found that this control method performs well in mitigating the vortex-induced

vibration (VIV). Also, the smaller spacing ratio and the larger coverage rates lead to better VIV suppression.

Gozmen et al. (2013b) experimentally controlled the vortex shedding behind a circular obstacle in shallow water using a splitter plate located in the downstream region at a Reynolds number of 6.25×10^3. They found that the turbulent quantities and mean flow, change significantly with length and height ratios of the splitter plates in shallow flow. Also, it is shown that L/D ration of 2, where D is cylinder diameter and L is splitter plate length, provides optimum control. Weickgenannt and Monkewitz (2000) controlled experimentally the vortex shedding in an axisymmetric bluff body wake by using a control disc mounted at the rear of an axisymmetric blunt-based body of revolution for the Reynolds number range $3.0 \times 10^3 < \mathrm{Re} < 5.0 \times 10^4$. El-Gammal et al. (2007) controlled the vortex shedding in a sectional bridge model by a spanwise sinusoidal perturbation method (SPPM). The same amplitude with two different SPPM configurations and two different wavelengths were used in this study. Their results showed that the SPPM with the higher wave steepness distinctively suppresses the vortex-induced vibrations (VIV). Ozono (2003) experimentally controlled the flow around a circular obstacle by using a few interference elements shifted along the wake. These elements were short and long splitter-plates and a circular cylinder. They found that the spectral peak associated with the vortex shedding weakens by using splitter-plates. Also, a base suction was created by shifting the downstream cylinder to upstream direction in two-cylinder case. Shi et al. (2010) experimentally investigated the effects of wall proximity on the characteristics of the wake downstream a 2-D square obstacle for a turbulent regime. They found that the time-averaged streamwise velocity in the wake region modifies significantly with the reduction in the gap width between the cylinder and the wall.

Finally, this method could be classified as both active and passive methods. Moreover, this method is classified in the group of wake control methods. This method is important from two viewpoints. First, the existence of applying an external element modifies the velocity profiles in the wake region of the bluff body and changes their stability nature. Second, applying external element alters the pressure and shear stress distributions in the wake region. This method may create undesirable forces due to the use of external body. Moreover, the performance of this method is very sensitive to the element arrangements such as the distance between the element and main bluff body and the placement of element with respect to the incoming flow.

Table 10 summarizes the researches on application of external element to control the vortex shedding and flow separation of a bluff body. Vortex induced vibration is a basic reason for the fatigue damage of deepwater risers and free spanning submarine pipelines. This phenomenon has received more attention during recent years due to the increase in exploration and extraction of offshore oil and gas resources. Utilizing a control rod is shown to be very good method to suppress the vortex induced vibration of deepwater drilling riser with a large aspect ratio, see e.g. Wu et al. (2012). In practical ocean engineering cases, multiple auxiliary pipelines are often available. Most of the previous studies in this method (Control rod) have used a single control rod, and studies on the use of multiple control rods cases are very limited. Finally, it should be noted that it is not practical to apply external elements as an integral part of the main configuration.

3. Energetic efficiency of control methods

The cost, energetic efficiency and optimization analyses of each active control method are significant parameters that are considered to evaluate and compare the various techniques. A key factor of an optimal flow control method is the minimization of input energy required for this method see e.g. Rashidi et al. (2011a), Rashidi et al. (2011b), Rashidi et al. (2014), and Rashidi et al. (2016). Such analyses help ocean engineers to select the most applicable and efficient method. In this section, recent studies in this field are reviewed. Choi et al. (2008) defined the control efficiency as the ratio of the save power to the control input power for the case of drag reduction. Recently a new parameter, namely Power Loss Coefficient, has been proposed to quantify the energetic efficiency. Power loss coefficient is employed for optimal PID control and it obtains the amount of the energy lost in the wake of the translating body. It is applicable to different flow configurations including active drag reduction, self-propulsion and thrust generation, see Arakeri and Shukla, (2013); Shukla and Arakeri (2013) determined the proper tangential velocity profiles which would result in minimum values of the drag force acting on the cylindrical body, and subsequently, minimum value of the net power consumption. They concluded that the flow tangential velocity enables energetically efficient propulsion. Das et al. (2016) proposed an energetically efficient active flow control strategy (PID) to control the wake vortices behind a circular cylinder. They used a linear quadratic optimal control formulation to minimize the cost functional. Their results showed that this system was energetically efficient, even when the twin eddies are still persisting behind the obstacle. Jukes and Choi (2009) optimally modified the vortex shedding cycle behind a circular cylinder by using a short plasma excitation. They expressed the effectiveness of plasma in reducing drag in terms of the energy efficiency. They concluded that a power saving ratio over 1000 can be achieved, while the energy efficiency was 51%. Note that the power saving ratio was defined as a ratio of the power saved by drag reduction to the fluidic power introduced by the plasma.

Table 11 summarizes researches performed on different algorithms to achieve an optimal control approach. Reynolds number, type of optimal target, and quantity of optimized parameters for each research are included in this table. As shown in this table, the optimization analyses are very limited for higher Reynolds numbers ($\mathrm{Re} > 1.0 \times 10^5$) and three-dimensional flows that are more applicable in ocean engineering. However, most attentions are focused on rotary oscillation control method and other methods, especially MHD and thermal methods, are needed to perform such analysis. Finally, an economic analysis is strongly advised, especially for experimental works to obtain the risks and gains of each technique. Such analysis has not been performed in previous works.

4. Drag analysis

An important factor, which should be considered for assessing different control techniques, is the effectiveness of each technique on the drag reduction. Table 12 presents a compilation of the available data on the impact of these techniques on the drag reduction. Note that the maximum drag reductions are presented in this table for each relevant method. As shown in this table, some methods, such as suction and blowing, external element (especially splitter plate), rotationally oscillating, and surface roughness are more active for drag reduction. Some other techniques need more attentions. For example, none of researches about thermal method, except the study of Chatterjee and Sinha (2014) have focused on the effects of heating on drag and lift forces. Note that some of these methods have both positive and negative impacts on the drag reduction. For example, Chatterjee and Sinha (2014) stated that heating can leads to drag reduction for lower heating flux, while it shows some opposite behavior for higher heating flux. There is a similar trend for MHD method. Singha and

Table 10
Researches on application of external element to control the vortex shedding and flow separation of a bluff body.

Authors	Type of research	Type of fluid	Reynolds number	Spatial dimensions	Classification	Controlled device	Controller
Strykowski and Sreenivasan (1990)	Experimental/ Numerical	Air/water	$30-1.2\times10^2$	2D	Passive	Circular cylinder	Small non-rotating circular cylinder
Nishiyama et al. (1991)	Experimental	Air	4.0×10^3–8.0×10^3	–	Active	Elliptic cylinder	Elliptic vibrating cylinder
Miau et al. (1993)	Experimental	Air	$5.3\times10^3-4.5\times10^4$	–	Passive	Trapezoidal cylinder	Splitter plate
Kwon and Choi (1996)	Numerical	Unknown	$80-1.6\times10^2$	2D	Passive	Circular cylinder	Splitter plate
Lee and Kim (1997)	Experimental	Air	$5.0\times10^3-5.0\times10^4$	–	Passive	Two circular cylinder	Three helically wrapped small rubber wires
Weickgenannt and Monkewitz (2000)	Experimental	Air	3.0×10^3–5.0×10^4	–	Passive	Axisymmetric blunt-based body	Disc
Mittal (2001)	Numerical	Unknown	1.0×10^2 and 1.0×10^4	2D	Active	Circular cylinder	Rotating cylinder
Mittal and Raghuvansh (2001)	Numerical	Unknown	$60-1.0\times10^2$	2D	Passive	Circular cylinder	Small non-rotating circular cylinder
Patnaik and Wei (2002)	Numerical	Unknown	2.0×10^2–4.0×10^2	2D	Active	D shape cylinder	Two small rotating circular cylinders
Ozono (2003)	Experimental	Air	$6.7\times10^3-2.5\times10^4$	–	Passive	Circular cylinder	Short or long splitter-plate or circular cylinder
Akilli et al. (2005)	Experimental	Water	5.0×10^3	–	Passive	Circular cylinder	Splitter plate
Kuo and Chen (2009)	Numerical	Unknown	80	2D	Passive	Circular cylinder	Two fixed circular cylinders
Muddada and Patnaik (2010)	Numerical	Unknown	1.0×10^2–3.0×10^2	2D	Active	Circular cylinder	Two rotating cylinder+feedback
Shi et al. (2010)	Experimental	Air	1.32×10^4	–	Passive	Square cylinder	Plane wall
Korkischko and Meneghini (2012)	Experimental	Water	3×10^3	–	Active	Circular cylinder	Two small rotating circular cylinders
Wu et al. (2012)	Experimental	Water	2.4×10^2–7.6×10^2	–	Passive	Slender riser	Multiple rods
Oruc (2012)	Experimental	Water	5.2×10^3	–	Passive	Circular cylinder	Screen
Bao and Tao (2013)	Numerical	Air	$20-1.6\times10^2$	2D	Passive	Circular cylinder	Parallel dual plates
Chen and Shao (2013)	Numerical+Experimental	Water	$75-1.3\times10^2$	2D	Passive	Rectangular cylinder	Small elements of circular, square, triangular and thin-strip cross-sections
Gozmen et al. (2013b)	Experimental	Water	6.25×10^3	–	Passive	Circular cylinder	Splitter plate
Vilaplana et al. (2013)	Experimental	Air	3.3×10^4	3D	Passive	Sphere	Small sphere
Reddy et al. (2013)	Analytically	Unknown	100	2D	Active	Circular cylinder	Two counter-rotating cylinders
Huera-Huarte (2014)	Experimental	Water	1.0×10^3–8.0×10^3	–	Passive	Circular cylinder	Splitter plate
Maiti and Bhatt (2014)	Numerical	Unknown	1.25×10^2–2×10^2	2D	Passive	Square cylinder	Rectangular cylinders and plane wall
Ozkan and Akilli (2014)	Experimental	Water	5.0×10^3	–	Passive	Circular cylinder	Attached permeable plates
Zhu and Yao (2015)	Numerical	Water	1.16×10^3–6.4×10^3	2D	Passive	Circular cylinder	Rods

Table 11
Recent researches on different algorithms to achieve an optimal control approach.

Authors	Reynolds number	Optimized parameter	Quantity of optimized parameters	Spatial dimensions
Rotary				
He et al. (2000)	2.0×10^2–6.0×10^2	Drag	60% reduction in drag	2D
Homescu et al. (2002)	$60-1.0\times10^3$	Drag	Unknown	2D
Protas and Styczek (2002)	75 and 1.5×10^2	Power drag+ Power control	93% reduction in drag	2D
Bergmann et al. (2005)	2.0×10^2	Drag	25% reduction in drag	2D
Sengupta et al. (2007)	1.5×10^4	Drag	66% reduction in drag	2D
Shukla and Arakeri (2012)	1–300	Drag	77% reduction in drag	2D
Arakeri and Shukla (2013)	100	Drag	79% reduction in drag	2D
Flinois and Colonius (2015)	$75-2.0\times10^2$	Power drag+ Power control	19% reduction in drag	2D
Feedback control				
Min and Choi (1999)	1.0×10^2 and 1.6×10^2	Drag/Lift	28% reduction in drag	2D
Leclerc et al. (2006)	1.0×10^2	Drag/Lift	12% reduction in drag	2D
Joe et al. (2009)	3.0×10^2	Lift	85% augmentation in lift	2D
Das et al. (2016)	100	Power loss coefficient	Unknown	2D
Blowing/suction				
Li et al. (2003)	1.1×10^2	Objective functional (a function of the initial condition, the model parameters, and the boundary parameter)	47% reduction in objective functional	2D
EHD				
Jukes and Choi (2009)	15,000	Drag/Lift	8% reduction in drag/50% augmentation in lift	3D
D'Adamo et al. (2011)	2.0×10^2	Energy consumption of EHD	Not mentioned	2D

Table 12
A compilation on available data about the impact of the control methods on the drag reduction.

Author	Relative drag reduction	Range of Reynolds number	Method
Thomas et al. (2005)	90%	1.28×10^4–2.54×10^4	Steady blowing with two actuators on a cylinder
Amitay et al. (1997)	30%	7.55×10^4	Synthetic jets
Sohankar et al. (2015)	72%	$70-1.5\times10^2$	Uniform suction and blowing
Delaunay and Kaiktsis (2001)	14%	<90	Steady base suction and blowing
Joseph et al. (2013)	10%	1.1×10^6–2.8×10^6	Micro-jets
Mimeau et al. (2014)	30%	$5.5\times10^2-3.0\times10^3$	Porous coatings
Muddada and Patnaik (2010)	53%	1.0×10^2–3.0×10^2	Two rotating cylinder+feedback
Lee et al. (2004)	29%	2.0×10^4	Small control rod installed upstream
Kuo and Chen (2009)	5%	80	Two fixed circular cylinders
Hwang et al. (2003)	23%	$30-1.6\times10^2$	Detached splitter plate
Gu et al. (2012)	30%	3.0×10^4–6.0×10^4	Rotatable splitter plates
Bao and Tao (2013)	23%	$20-1.6\times10^2$	Parallel dual plates
Korkischko and Meneghini (2012)	60%	3.0×10^3	Two small rotating circular cylinders
Bearman and Owen (1998)	30%	4.0×10^4	Spanwise sinusoidal forms and with sinusoidal front faces
He et al. (2000)	60%	2.0×10^2–6.0×10^2	Rotationally oscillating
Tokumaru and Diimotakis (1989)	80%	1.5×10^4	Rotationally oscillating
S.J. Lee and J.Y. Lee (2006)	32.82%	4.14×10^3	Rotationally oscillating
Bergmann et al. (2005)	25%	2.0×10^2	Rotationally oscillating
Sengupta et al. (2007)	66%	1.5×10^4	Rotationally oscillating
Kim and Choi (2005)	23%	$40-3.9\times10^3$	Blowing and suction from the slots placed at upper and lower surfaces of the obstacle
Huang et al. (2007)	25%	3×10^4–4×10^5	Surface roughness
Zhou et al. (2015)	30%	6.0×10^3–8×10^4	Surface roughness
Singha and Sinhamahapatra (2011)	4%	$50-2.5\times10^2$	MHD
Chen and Aubry (2005)	46%	2.0×10^2	MHD
Min and Choi (1999)	28%	1.0×10^2 and 1.6×10^2	Feedback
Leclerc et al. (2006)	12%	1.0×10^2	Feedback
He et al. (2000)	60%	2.0×10^2–6.0×10^2	Rotationally oscillating
Protas and Styczek (2002)	93%	75 and 1.5×10^2	Rotationally oscillating
Bergmann et al. (2005)	25%	2.0×10^2	Rotationally oscillating
Sengupta et al. (2007)	66%	1.5×10^4	Rotationally oscillating
Flinois and Colonius (2015)	19%	$75-2.0\times10^2$	Rotationally oscillating

Sinhamahapatra (2008) showed that the mean drag coefficient decreases slowly for lower magnetic field strength and increases rapidly for higher magnetic field strength. It is worth mentioning that some researchers used two very simple passive techniques to control the vortex shedding and especially reduce the drag coefficient. First technique applies small tabs on the lower and upper trailing edges of the bluff bodies (Park et al., 2006). This leads to perturb the wake, subsequently attenuate the vortex shedding,

and decrease in drag coefficient. Park et al. (2006) examined both experimentally and numerically this technique successfully for the Reynolds number in the range of 2.0×10^4 to 8.0×10^4. As second technique, some researchers used wavy walls for bluff bodies to suppress the vortex shedding and decrease the drag coefficient. For example, Darekar and Sherwin (2001) used in a numerical study the wavy stagnation face for flow around a square cylinder at low Reynolds numbers in the range of 10-1.5×10^2. They found that this technique leads to suppression of the vortex shedding by the spanwise waviness and subsequently a significant reduction in drag coefficient. In another research, Xu et al. (2014) applied traveling wave wall for a circular cylinder to reduce the drag coefficient and suppress the vortex-induced vibration. They performed a numerical study for a fixed low Reynolds number (i.e. $Re = 2.0 \times 10^2$). They presented that this control technique can leads to reduction in the fluctuation of the lift and drag coefficients. As a result, these low cost and simple techniques can be used to reduce the drag coefficient and control of flow around the bluff bodies. As a result, the drag coefficient significantly decreases (up to 90%) by using some methods such as rotationally oscillating or steady blowing with two actuators on a cylinder.

5. Summary and concluding remarks

This paper focused on reviews of the vortex shedding suppression and wake control. Some of the applications of these methods are summarized in Table 13.

Several existing approaches and techniques used to control the wake destructive behavior and suppression of vortex shedding behind bluff bodies are discussed and reviewed. These techniques are classified into nine categories based on the fundamental methods and applications utilized. The following conclusions and suggestions can be drawn:

- We presented the ranges of Reynolds number that were used by researchers for each category of control technique. However, some techniques work better for special flow regimes and some are suitable for wider flow regimes. As an example, surface roughness approach works well at subcritical Reynolds numbers ($Re = 1 \times 10^3$ to 1×10^4) but does not work at lower values of Reynolds number, see e.g. Achenbach, 1971. For low values of Reynolds number that have applications in microsystems, the following methods have been tested successfully: Splitter plates, second (control) cylinder, thermal method, secondary flow (base bleed and suction), permeable wall, feedback control law based on a single-sensor measurement, cylinder rotation or transverse oscillations, and apply of steady magnetic fields.
- Most of the researches in the literature and reviewed here, are performed for a single bluff body, while in practice, vertical cylinder and structures exist in groups. Oil and gas transmission lines in the oceans and other marine pipelines, vertical columns of offshore platforms, and heat exchanger tube bundles are a few examples of this application.
- Some type of oscillation, such as the flow perturbations and imposed sound field, have not received a full attention and hence have good potential for future researches. These types of control methods are more applicable in ocean engineering.
- The future attentions should be more focused on modifying the near wake flow and vortex shedding to use them as the advantage instead of effort for removing them completely.
- There are some technologies such as micro-electro-mechanical systems (MEMS) to miniaturize the synthetic jet. Such technologies lead to save the power needed for controlling the flow.
- A very good method to suppress the vortex induced vibration of deepwater drilling riser with a large aspect ratio is the use of a control rod. In practical ocean engineering cases, multiple auxiliary pipelines are often available. Most of the previous studies in this field (Control rod) have used a single control rod, and studies using multiple control rods cases are very limited.
- A good method for controlling the wake turbulence behind an obstacle could be angular momentum injection as tested successfully by researchers. They showed that the wake turbulence could be completely suppressed. This method has a good potential for future researches as it works well for turbulent flows.
- Distributed force in spanwise direction to flow over a bluff body modifies the vertical evolution in the wake and leads to drag reduction significantly for laminar and turbulent flows. This force can produce by blowing, suction, perturbations, and phase excitation by surface heaters.
- In summary, the target of control methods in boundary layer classification are to prevent or provoke boundary layer separation, control the spanwise and streamwise vortices in a turbulent boundary layer, transition delay, and decrease the skin-friction drag. Subsequently, the purposes of wake control methods are to supress the pressure drag and control the wake structures, and the pressure distribution on the rear portion of cylinders.
- With regards to VIV oscillation control, and before selecting the control method, note that higher quantum of control is required for objects in water than in air, due to the damping effects.
- The energetic efficiency and optimization analyses for each active control method must be considered to evaluate and compare the various techniques. Such analyses help ocean engineers to select the best method. Although, there are some researches about this topic, but most of the studies have focused on rotary oscillation control methods; other methods, especially MHD and thermal methods, are required such optimization analysis.
- An economic analysis is strongly advised especially for experimental works to obtain the risks and gains of each technique.

Table 13
Applications of existing approaches for vortex shedding suppression and wake control.

Name of method	Applications
EHD	This method is suitable for aerodynamic applications such as airfoils typically used in wind turbine blades, civil air traffic projects and aircraft.
External element	This method is used in ocean structures, bridges, high voltage lines, deepwater risers and free spanning submarine pipelines, flourishing extraction of ocean oil and gas resources.
Feedback control	This method is used in aircraft and projectile aerodynamics include dynamic stall control, marine structures, chemical mixing improvement, submarine periscopes, increase mixing and heat transfer in combustion, and civil and engineering applications.
MHD	This method can be used to control the flow over ship hull, tubular heat exchangers, pipelines, suspension wires, oblique shocks and suspension bridges.
Rotary oscillations	This method can be used to control the flow for tube heat exchangers, shafts, drilling of oil wells, nuclear reactor fuel rods and steel suspension bridge cables.
Secondary flow	These techniques are used in long-span suspension bridges and cable-stayed bridges.
Surface roughness	This method is utilized in offshore and marine application, such as platform pillars, pipelines and risers.
Thermal effects	As a natural mean to control the boundary layer separation over a cylinder, it can be used in many engineering applications.

Such analysis has not been performed in previous works.

- The transition of flow pass a bluff body from 2D to 3D is an important phenomenon to understand in an engineering context because the wake-induced forces can have potentially detrimental structural or local effects on the bodies or their surroundings. The effects of aforesaid method on this transition have a good potential for future studies.
- Applying zero-mass-flux actuator types, which need little energy, is a remarkable method for further investigations in the field of flow control around bluff bodies.
- New optical technologies in flow visualization especially in the wake region include the laser-induced fluorescence and particle-image-velocimetry, are advised to be used as they are tested successfully by some researches, Lee and Lee (2008).
- There are two very simple passive techniques to control the vortex shedding and especially reduce the drag coefficient. Small tabs are applied on the lower and upper trailing edges of the bluff bodies as first technique. For second technique, some researchers used wavy walls for bluff bodies to suppress the vortex shedding and decrease the drag coefficient.
- The researches in this field should be extended to a pragmatic approach. Such approach covers other disciplines including the noise, structures, and systems integration.
- Developments in smart sensors and actuators with their integration into active flow control methods are interesting solutions for minimizing the objective functional.
- Microelectro mechanical systems can be used to reduce the drag coefficient and control the flow separation.
- Piezo-electric can be used as a new actuation for controlling the flow.
- Development of low-order models, such as Galerkin model, can be useful for the suppression of vortex shedding.

References

Achenbach, E., 1971. Influence of surface roughness on the cross-flow around a circular cylinder. J. Fluid Mech. 46 (2), 321–335.

Achenbach, E., Heinecke, A., 1981. On vortex shedding from smooth and rough cylinders in the range of Reyonlds numbers 6×10^3 to 5×10^6. J. Fluid Mech. 109, 239–251.

Akilli, H., Sahin, B., Filiz Tumen, N., 2005. Suppression of vortex shedding of circular cylinder in shallow water by a splitter plate. Flow Meas. Instrum. 16, 211–219.

Allen, D.W., Henning, D.L., Surface roughness effects on vortex-induced vibration of cylindrical structures at critical and supercritical Reynolds numbers, 2001. In: Proceedings of the Offshore Technology Conference, Houston, Texas, USA OTC, p. 13302.

Amitay, M., Honohan, A., Trautman, M., Glezer, A., 1997. Modification of the aerodynamic characteristics of bluff bodies using fluidic actuators. In: Proceedings of the 28th Fluid Dynamics Conference, Fluid Dynamics and Co-located Conferences.

Arakeri, J.H., Shukla, R.K., 2013. A unified view of energetic efficiency in active drag reduction, thrust generation and self-propulsion through a loss coefficient with some applications. Journal of Fluids and Structures 41, 22–32.

Armstrong, B.J., Barnes, F.H., Grant, I., 1986. The effect of a perturbation on the flow over a cylinder. Phys. Fluids 29, 2095–2102.

Artana, G., Sosa, R., Moreau, E., Touchard, G., 2003. "Control of the near-wake flow around a circular cylinder with electrohydrodynamic actuators.". Exp. Fluids 35, 580–588.

Baek, S.J., Sung, H.J., 1998. Numerical simulation of the flow behind a rotary oscillating circular cylinder. Phys. Fluids 10 (4), 869–876.

Bao, Y., Tao, J., 2013. The passive control of wake flow behind a circular cylinder by parallel dual plates. J. Fluids Struct. 37, 201–219.

Baz, A., Ro, J., 1991. Active control of flow-induced vibrations of a flexible cylinder using direct velocity feedback. J. Sound Vib. 146 (1), 33–45.

Bearman, P.W., Harvey, J.K., 1993. Control of circular cylinder flow by the use of dimples. AIAA J. 31 (10), 1753–1756.

Bearman, P.W., Owen, J.C., 1998. Reduction of bluff-body drag and suppression of vortex shedding by the introduction of wavy separation lines. J. Fluids Struct. 12, 123–130.

Beaudoin, J.F., Cadot, O., Aider, J.L., Wesfreid, J.E., 2006. Bluff-body drag reduction by extremum-seeking control. J. Fluids Struct. 22, 973–978.

Becker, R., King, R., 2006. Adaptive closed-loop separation control on a high-lift configuration using extremum seeking. In: Proceedings of the 3rd AIAA Flow Control Conference 5-8 June 2006, San Francisco, California.

Berger, E., 1967. Suppression of vortex shedding and turbulence behind oscillating cylinders. Phys. Fluids 10, S191–S193.

Bergmann, M., Cordier, L., Brancher, J.P., 2005. Optimal rotary control of the cylinder wake using proper orthogonal decomposition reduced-order model. Phys. Fluids 17 (9), 097101.

Bernitsas, M.M., Raghavan, K., 2008. Reduction/suppression of VIV of circular cylinders through roughness distribution at $8 \times 10^3 < \mathrm{Re} < 2.0 \times 10^5$. In: Proceedings of the Offshore Mechanics and Arctic Engineering Conference, Estoril, Portugal, OMAE, pp. 58024.

Bernitsas, M.M., Raghavan, K., Duchene, G., 2008. Induced separation and vorticity using roughness in VIV of circular cylinders at $8 \times 10^3 < \mathrm{Re} < 2.0 \times 10^5$. In: Proceedings of the Offshore Mechanics and Arctic Engineering Conference, Estoril, Portugal, OMAE, pp. 58023.

Bimbato, A.M., Alcântara Pereira, L.A., Hiroo Hirata, M., 2013. Suppression of vortex shedding on a bluff body. J. Wind Eng. Ind. Aerodyn. 121, 16–28.

Blevins, R.D., 1985. The effect of sound on vortex shedding from cylinder. Phys. Fluids 161, 217–237.

Bovand, M., Rashidi, S., Esfahani, J.A., 2015a. Enhancement of heat transfer by nanofluids and orientations of the equilateral triangular obstacle. Energy Convers. Manag. 97, 212–223.

Bovand, M., Rashidi, S., Dehghan, M., Esfahani, J.A., Valipour, M.S., 2015c. Control of wake and vortex shedding behind a porous circular obstacle by exerting an external magnetic field. J. Magn. Magn. Mater. 385, 198–206.

Carini, M., Pralits, J.O., Luchini, P., 2015. Feedback control of vortex shedding using a full-order optimal compensator. J. Fluids Struct. 53, 15–25.

Chaligné, S., Castelain, T., Michard, M., Chacaton, D., Juvé, D., 2014. Fluidic control of wake-flow behind a two-dimensional square back bluff body. Comptes Rendus Méc. 342, 349–355.

Chan, A.S., Dewey, P.A., Jameson, A., Liang, C., Smits, A.J., 2011. Vortex suppression and drag reduction in the wake of counter-rotating cylinders. J. Fluid Mech. 679, 343–382.

Chang, C.C., Kumar, R.A., Bernitsas, M.M., 2011. VIV and galloping of single circular cylinder with surface roughness at $3.0 \times 10^4 < \mathrm{Re} < 1.2 \times 105$. Ocean Eng. 38, 1713–1732.

Chatterjee, D., 2014. Dual role of thermal buoyancy in controlling boundary layer separation around bluff obstacles. Int. Commun. Heat Mass Transf. 56, 152–158.

Chatterjee, D., Ray, S., 2014. Influence of thermal buoyancy on boundary layer separation over a triangular surface. Int. J. Heat Mass Transf. 79, 769–782.

Chatterjee, D., Mondal, B., 2014. Control of flow separation around bluff obstacles by superimposed thermal buoyancy. Int. J. Heat Mass Transf. 72, 128–138.

Chatterjee, D., Sinha, C., 2014. Influence of thermal buoyancy on vortex shedding behind a rotating circular cylinder in cross flow at subcritical Reynolds numbers. J. Heat Transf. 136, 051704-1.

Chatterjee, D., Chatterjee, K., Mondal, B., 2012. Control of flow separation around bluff obstacles by transverse magnetic field. ASME J. Fluids Eng. 134, 091102-1.

Chen, W.L., Xin, D.B., Xu, F., Li, H., Ou, J.P., Hu, H., 2013. Suppression of vortex-induced vibration of a circular cylinder using suction-based flow control. J. Fluids Struct. 42, 25–39.

Chen, Y.J., Shao, C.P., 2013. Suppression of vortex shedding from a rectangular cylinder at low Reynolds numbers. J. Fluids Struct. 43, 15–27.

Chen, Z., Aubry, N., 2005. Active control of cylinder wake. Commun. Nonlinear Sci. Numer. Simul. 10, 205–216.

Choi, H., Jeon, W.P., Kim, J., 2008. Control of flow over a bluff body. Annu. Rev. Fluid Mech. 40, 113–139.

D'Adamo, J., Sosa, R., Barcelo, M., Artana, G., 2011. Wake flow stabilization with DBD plasma actuators for low re numbers. J. Phys. Conf. Ser. 296 (1), 1–11.

Darekar, R.M., Sherwin, S.J., 2001. Flow past a square-section cylinder with a wavy stagnation face. J. Fluid Mech. 426, 263–295.

Das, P.K., Mathew, S., Shaiju, A.J., Patnaik, B.S.V., 2016. Energetically efficient proportional-integral differential (PID) control of wake vortices behind a circular cylinder. Fluid Dyn. Res. 48, 015510.

Delaunay, Y., Kaiktsis, L., 2001. Control of circular cylinder wakes using base mass transpiration. Phys. Fluids 13, 3285–3301.

El-Gammal, M., Hangan, H., King, P., 2007. Control of vortex shedding-induced effects in a sectional bridge model by spanwise perturbation method. J. Wind Eng. Ind. Aerodyn. 95, 663–678.

Feng, L.H., Wang, J.J., 2010. Circular cylinder vortex-synchronization control with a synthetic jet positioned at the rear stagnation point. J. Fluids Mech. 662, 232–259.

Feng, L.H., Wang, J.J., Pan, C., 2010. Effect of novel synthetic jet on wake vortex shedding modes of a circular cylinder. J. Fluids Struct. 26, 900–917.

Feng, L.H., Wang, J.J., Pan, C., 2011. Proper orthogonal decomposition analysis of vortex dynamics of a circular cylinder under synthetic jet control. Phys. Fluids 23, 014106-1-13.

Flinois, T.L.B., Colonius, T., 2015. Optimal control of circular cylinder wakes using long control horizons. Phys. Fluids 27, 087105.

Fu, H., Rockwell, D., 2005. Shallow flow past a cylinder: control of the near wake. J. Fluid Mech. 539, 1–24.

Fujisawa, N., Nakabayashi, T., 2002. Neural network control of vortex shedding from a circular cylinder using rotational feedback oscillations. J. Fluids Struct. 16, 113–119.

Fujisawa, N., Kawaji, Y., Ikemoto, K., 2001. Feedback control of vortex shedding from a circular cylinder by rotational oscillations. J. Fluids Struct. 15, 23–37.

Gad-el-Hak, M., Bushnell, D.M., 1991. Separation control: review. J. Fluids Eng. 113, 5–30.

Gao, Y., Fu, S., Wang, J., Song, L., Chen, Y., 2015. Experimental study of the effects of

surface roughness on the vortex-induced vibration response of a flexible cylinder. Ocean Eng. 103, 40–54.
Gozmen, B., Akilli, H., Sahin, B., 2013a. Vortex control of cylinder wake by permeable cylinder. Çukurova Univ., J. Fac. Eng. Archit. 28, 77–85.
Gozmen, B., Akilli, H., Sahin, B., 2013b. Passive control of circular cylinder wake in shallow flow. Measurement 46, 1125–1136.
Graham, C., Huang, P., 2010. Analysis of a Passive Flow Control Device via Flow Visualization Techniques. A Thesis for BS in Aerospace Engineering. California Polytechnic State University, Spring.
Gu, F., Wang, J.S., Qiao, X.Q., Huang, Z., 2012. Pressure distribution, fluctuating forces and vortex shedding behavior of circular cylinder with rotatable splitter plates. J. Fluids Struct. 28, 263–278.
He, J.W., Glowinski, R., Metcalfe, R., Nordlander, A., Périaux, J., 2000. Active control and drag optimization for flow past a circular cylinder. Part 1. Oscillatory cylinder rotation. J. Comput. Phys. 163, 83–117.
Hiejima, S., Kumao, T., Taniguchi, T., 2005. Feedback control of vortex shedding around a bluff body by velocity excitation. Int. J. Comput. Fluid Dyn. 19, 87–92.
Homescu, C., Navon, I.M., Li, Z., 2002. Suppression of vortex shedding for flow around a circular cylinder using optimal control. Int. J. Numer. Methods Fluids 38 (1), 43–69.
Huang, S., 2011. VIV suppression of a two-degree-of-freedom circular cylinder and drag reduction of a fixed circular cylinder by the use of helical grooves. J. Fluids Struct. 27, 1124–1133.
Huang, X.Y., 1995. Suppression of vortex shedding from a circular cylinder by internal acoustic excitation. J. Fluids Struct. 9, 563–570.
Huang, X.Y., 1996. Feedback control of vortex shedding from a circular cylinder. Exp. Fluids 20, 218–224.
Huang, S. Clelland, D., Day, S., James, R., 2007. Drag reduction of deepwater risers by the use of helical grooves. In: International conference on offshore mechanics & arctic engineering.
Huera-Huarte, F.J., 2014. On splitter plate coverage for suppression of vortex-induced vibrations of flexible cylinders. Appl. Ocean Res. 48, 244–249.
Hwang, J.Y., Yang, K.S., Sun, S.H., 2003. Reduction of flow-induced forces on circular cylinder using a detached splitter plate. Phys. Fluids 15 (8), 2433–2436.
Hyun, K.T., Chun, C.H., 2003. The wake flow control behind a circular cylinder using ion wind. Exp. Fluids 35, 541–552.
Joe, W.T., Colonius, T., MacMynowski, D.G., 2009. Optimized waveforms for feedback control of vortex shedding. In: Proceedings of the 39th AIAA Fluid Dynamics Conference, June 2009, San Antonio, Texas.
Joseph, P., Edouard, C., Amandolese, X., Aider, J.L., 2013. Flow control using MEMS pulsed micro-jets on the Ahmed body. Exp. Fluids 54, 1–12.
Jukes, T.N., Choi, K.S., 2009. Long lasting modifications to vortex shedding using a short plasma excitation. Phys. Rev. Lett. 102, 254501.
Kim, J., Choi, H., 2005. Distributed forcing of flow over a circular cylinder. Phys. Fluids 17, 0331031-16.
King, R., 1997. A review of vortex shedding research and its application. Ocean Eng. 4, 141–171.
Kiu, K.Y., Stappenbelt, B., Thiagarajan, K.P., 2011. Effects of uniform surface roughness on vortex-induced vibration of towed vertical cylinders. J. Sound Vib. 330, 4753–4763.
Korkischko, I., Meneghini, J.R., 2012. Suppression of vortex-induced vibration using moving surface boundary-layer control. J. Fluids Struct. 34, 259–270.
Kumar, R.A., Sohn, C.H., Gowda, B.H.L., 2008. Passive control of vortex-induced vibrations: an overview. Recent Pat. Mech. Eng. 1, 1–11.
Kunze, S., Brücker, C., 2012. Control of vortex shedding on a circular cylinder using self-adaptive hairy-flaps. C. R. Mec. 340, 41–56.
Kuo, C.H., Chen, C.C., 2009. Passive control of wake flow by two small control cylinders at Reynolds number 80. J. Fluids Struct. 25, 1021–1028.
Kwon, K., Choi, H., 1996. Control of laminar vortex shedding behind a circular cylinder using splitter plates. Phys. Fluids 8, 479–486.
Layek, G.C., Midya, C., Gupta, A.S., 2008. Influences of suction and blowing on vortex shedding behind a square cylinder in a channel. Int. J. Non-Linear Mech. 43, 979–984.
Leclerc, E., Sagaut, P., Mohammadi, B., 2006. On the use of incomplete sensitivities for feedback control of laminar vortex shedding. Comput. Fluids 35, 1432–1443.
Lecordier, J.C., Hamma, L., Paranthoen, P., 1991. The control of vortex shedding behind heated circular cylinders at low Reynolds numbers. Exp. Fluids 10, 224–229.
Lecordier, J.C., Browne, L.W.B., Le Masson, S., Dumouchel, F., Paranthoen, P., 2000. Control of vortex shedding by thermal effect at low Reynolds numbers. Exp. Therm. Fluid Sci. 21, 227–237.
Lee, S., Kim, H., 1997. The effect of surface protrusions on the near wake of a circular cylinder. J. Wind Eng. Ind. Aerodyn. 69–71, 351–361.
Lee, S.J., Lee, J.Y., 2006. Flow structure of wake behind a rotationally oscillating circular cylinder. J. Fluids Struct. 22, 1097–1112.
Lee, S.J., Lee, J.Y., 2008. PIV measurements of the wake behind a rotationally oscillating circular cylinder. J. Fluids Struct. 24, 2–17.
Lee, S.J., Lee, S.I., Park, C.W., 2004. Reducing the drag on a circular cylinder by upstream installation of a small control rod. Fluid Dyn. Res. 34, 233–250.
Lei, C., Cheng, L., Armfield, S.W., Kavanagh, K., 2000. Vortex shedding suppression for flow over a circular cylinder near a plane boundary. Ocean Eng. 27, 1109–1127.
Li, Z., Navon, I.M., Hussaini, M.Y., Le Dimet, F.X., 2003. Optimal control of cylinder wakes via suction and blowing. Comput. Fluids 32, 149–171.
Liu, Y.G., Feng, L.H., 2015. Suppression of lift fluctuations on a circular cylinder by inducing the symmetric vortex shedding mode. J. Fluids Struct. 54, 743–759.
Lu, L., Qin, J.M., Teng, B., Li, Y.C., 2011. Numerical investigations of lift suppression by feedback rotary oscillation of circular cylinder at low Reynolds number. Phys. Fluids 23, 033601.
Maiti, D.K., Bhatt, R., 2014. Vortex shedding suppression and aerodynamic characteristics of square cylinder due to offsetting of rectangular cylinders towards a plane. Ocean Eng. 82, 91–104.
Miau, J.J., Yang, C.C., Chou, J.H., Lee, K.R., 1993. Suppression of low-frequency variations in vortex shedding by a splitter plate behind a bluff body. J. Fluids Struct. 7, 897–912.
Mimeau, C., Mortazavi, I., Cottet, G.H., 2014. Passive flow control around a semi-circular cylinder using porous coatings. Int. J. Flow Control 6, 15–21.
Min, C., Choi, H., 1999. Suboptimal feedback control of vortex shedding at low Reynolds numbers. J. Fluid Mech. 401, 123–156.
Mittal, S., 2001. Control of flow past bluff bodies using rotating control cylinders. J. Fluids Struct. 15, 291–326.
Mittal, S., Raghuvanshi, A., 2001. Control of vortex shedding behind circular cylinder for flows at low Reynolds numbers. Int. J. Numer. Method Fluids 35, 421–447.
Modi, V.J., 1997. Passive control of vortex-induced vibrations: an overview. J. Fluids Struct. 11, 627–663.
Muddada, S., Patnaik, B.S.V., 2010. An active flow control strategy for the suppression of vortex structures behind a circular cylinder. Eur. J. Mech. B/Fluids 29, 93–104.
Muddada, S., Patnaik, B.S.V., 2011. Application of chaos control techniques to fluid turbulence. Appl. Chaos Nonlinear Dyn. Eng., Part Ser. Underst. Complex Syst. 1, 87–136.
Muralidharan, K., Muddada, Sridhar, Patnaik, B.S.V., 2013. Numerical simulation of vortex induced vibrations and its control by suction and blowing. Appl. Math. Model. 37, 284–307.
Mutschke, G., Shatrov, V., Gerbeth, G., 1998. Cylinder wake control by magnetic fields in liquid metal flows. Exp. Therm. Fluid Sci. 16, 92–99.
Mutschke, G., Gerbeth, G., Albrecht, T., Grundmann, R., 2006. Separation control at hydrofoils using Lorentz forces. Eur. J. Mech. B/Fluids 25, 137–152.
Nakamura, Y., Tomonari, Y., 1982. The effect of surface roughness on the flow past circular cylinders at high Reynolds numbers. J. Fluid Mech. 123, 363–378.
Nati, G., Kotsonis, M., Ghaemi, S., Scarano, F., 2013. Control of vortex shedding from a blunt trailing edge using plasma actuators. Exp. Therm. Fluid Sci. 46, 199–210.
Nishiyama, H., Ota, T., Kon, N., 1991. Vortex shedding controlled by the transverse vibration of three in-line elliptic cylinders in a uniform flow. J. Wind Eng. Ind. Aerodyn. 37, 141–153.
Okajima, A., Nagamori, T., Matsunaga, F., Kiwata, T., 1999. Some experiments on flow-induced vibration of a circular cylinder with surface roughness. J. Fluids Struct. 13, 853–864.
Oruc, V., 2012. Passive control of flow structures around a circular cylinder by using screen. J. Fluids Struct. 33, 229–242.
Ozkan, G.M., Akilli, H., 2014. Flow control around bluff bodies by attached permeable plates. Int. J. Mech. Aerosp. Ind. Mechatron. Eng. 8, 1027–1031.
Ozkan, G.M., Oruc, V., Akilli, H., Sahin, B., 2012. Flow around a cylinder surrounded by a permeable cylinder in shallow water. Exp. Fluids 53 (6), 1751–1763.
Ozono, S., 2003. Vortex suppression of the cylinder wake by deflectors. J. Wind Eng. Ind. Aerodyn. 91, 91–99.
Park, D.S., Ladd, D.M., Hendricks, E.W., 1994. Feedback control of von Kármán vortex shedding behind a circular cylinder at low Reynolds numbers. Phys. Fluids 6, 2390–2405.
Park, H., Lee, D., Jeon, W.P., Hahn, S., Kim, J., Kim, J., Choi, J., Choi, H., 2006. Drag reduction in flow over a two-dimensional bluff body with a blunt trailing edge using a new passive device. J. Fluid Mech. 563, 389–414.
Patnaik, B.S.V., Wei, G.W., 2002. Controlling Wake Turbulence. Phys. Rev. Lett. 88 (5), 054502–054504.
Pinar, E., Ozkan, G.M., Durhasan, T., Aksoy, M.M., Akilli, H., Sahin, B., 2015. Flow structure around perforated cylinders in shallow water. J. Fluids Struct. 55, 52–63.
Posdziech, O., Grundmann, R., 2001. Electromagnetic control of seawater flow around circular cylinders. Eur. J. Mech. B/Fluids 20, 255–274.
Post, M.L., Corke, T.C., 2004. Separation control on high angle of attack airfoil using plasma actuators. AIAA J. 42 (11), 2177–2184.
Protas, B., Styczek, A., 2002. Optimal rotary control of the cylinder wake in the laminar regime. Phys. Fluids 14 (7), 2073.
Rashidi, A., Fathi, H., Brilakis, I., 2011a. Innovative stereo vision-based approach to generate dense depth map of transportation infrastructure, Transp. Res. Rec.:. J. Transp. Res. Board 2215, 93–99.
Rashidi, A., Jazebi, F., Brilakis, I., 2011b. Neurofuzzy genetic system for selection of construction project managers. ASCE J. Constr. Eng. Manag 137 (1), 17–29.
Rashidi, A., Rashidi-Nejad, H., Maghiar, M., 2014. Productivity estimation of bulldozers using generalized linear mixed models. KSCE J. Civil Eng. 18 (6), 1580–1589.
Rashidi, A., Sigari, M.H., Maghiar, M., Citrin, D., 2016. An analogy between various machinelearning techniques for detecting construction materials in digital images. KSCE J. Civil Eng. 20 (4), 1178–1188.
Rashidi, S., Esfahani, J.A., 2015e. The effect of magnetic field on instabilities of heat transfer from an obstacle in a channel. J. Magn. Magn. Mater. 391, 5–11.
Rashidi, S., Tamayol, A., Valipour, M.S., Shokri, N., 2013. Fluid flow and forced convection heat transfer around a solid cylinder wrapped with a porous ring. Int. J. Heat Mass Transf. 63, 91–100.
Rashidi, S., Bovand, M., Pop, I., Valipour, M.S., 2014a. Numerical simulation of forced convective heat transfer past a square diamond-shaped porous cylinder.

Transp. Porous Media 102 (2), 207–225.
Rashidi, S., Masoodi, R., Bovand, M., Valipour, M.S., 2014b. Numerical study of flow around and through a porous diamond cylinder with different apex angels. Int. J. Numer. Methods Heat Fluid Flow. 24 (7), 1504–1518.
Rashidi, S., Nouri-Borujerdi, A., Valipour, M.S., Ellahi, R., Pop, I., 2015a. Stress-jump and continuity interface conditions for a cylinder embedded in a porous medium. Transp. Porous Media 107 (1), 171–186.
Rashidi, S., Dehghan, M., Ellahi, R., Riaz, M., Jamal-Abad, M.T., 2015b. Study of stream wise transverse magnetic fluid flow with heat transfer around an obstacle embedded in a porous medium. J. Magn. Magn. Mater. 378, 128–137.
Rashidi, S., Bovand, M., Esfahani, J.A., Öztop, H.F., Masoodi, R., 2015c. Control of wake structure behind a square cylinder by Magnetohydrodynamics. ASME J. Fluids Eng. 137 (6), 061102–061108.
Reddy, M.S., Muddada, S., Patnaik, B.S.V., 2013. Flow past a circular cylinder with momentum injection: optimal control cylinder design. Fluid Dyn. Res. 45, 015501.
Ribeiro, L.J.D., 1991a. Effects of surface roughness on the two-dimensional flow past circular cylinders I: mean forces and pressures. J. Wind Eng. Ind. Aerodyn. 37 (3), 299–309.
Ribeiro, L.J.D., 1991b. Effects of surface roughness on the two-dimensional flow past circular cylinders II: fluctuating forces and pressures. J. Wind Eng. Ind. Aerodyn. 37 (3), 311–326.
Roussopoulos, K., 1993. Feedback control of vortex shedding at low Reynolds numbers. J. Fluid Mech. 24, 267–296.
Roussopoulos, K., Monkewitz, P.A., 1996. Nonlinear modelling of vortex shedding control in cylinder wakes. Phys. D: Nonlinear Phenom. 97, 264–273.
Seal, C.V., Smith, C.R., 1999. The control of turbulent end-wall boundary layers using surface suction. Exp. Fluids 27, 484–496.
Sengupta, T.K., Deb, K., Talla, S.B., 2007. Control of flow using genetic algorithm for a circular cylinder executing rotary oscillation. Comput. Fluids 36, 578–600.
Shi, L.L., Liu, Y.Z., Sung, H.J., 2010. On the wake with and without vortex shedding suppression behind a two-dimensional square cylinder in proximity to a plane wall. J. Wind Eng. Ind. Aerodyn. 98, 492–503.
Shih, W.C.L., Wangl, C., Coles, D., Roshko, A., 1993. Experiments on flow past rough circular cylinders at large Reynolds numbers. J. Wind Eng. Ind. Aerodyn. 49, 351–368.
Shmilovich, A., Yadlin, Y., 2011. Flow control techniques for transport aircraft. AIAA J. 49 (3), 489–502.
Shukla, R.K., Arakeri, J.H., 2013. Minimum power consumption for drag reduction on a circular cylinder by tangential surface motion. J. Fluid Mech. 715, 597–641.
Singha, S., Sinhamahapatra, K.P., 2011. Control of vortex shedding from a circular cylinder using imposed transverse magnetic field. Int. J. Numer. Methods Heat Fluid Flow 21 (1), 32–45.
Singha, S., Sinhamahapatra, K.P., Mukherjea, S.K., 2007. Control of vortex shedding from a bluff body using imposed magnetic field. ASME J. Fluids Eng. 129, 517–523.
Sohankar, A., Khodadadi, M., Rangraz, E., 2015. Control of fluid flow and heat transfer around a square cylinder by uniform suction and blowing at low Reynolds numbers. Comput. Fluids 109, 155–167.
Son, D., Jeon, S., Choi, H., 2011. A proportional–integral–differential control of flow over a circular cylinder. Philos. Trans. R. Soc. A 369, 1540–1555.
Straatman, A.G., Martinuzzi, R.J., 2002. A study on the suppression of vortex shedding from a square cylinder near a wall. Eng. Turbul. Model. Exp. 5, 403–411.
Strykowski, P.J., Sreenivasan, K.R., 1990. On the formation and suppression of vortex 'shedding' at low Reynolds numbers. J. Fluid Mech. 218, 71–107.
Sung, Y., Kim, W., Mungal, M.G., Cappelli, M.A., 2006. Aerodynamic modification of flow over bluff objects by plasma actuation. Exp. Fluids 41, 479–486.
Tao, J.S., Huang, X.Y., Chan, W.K., 1996. A flow visualization study on feedback control of vortex shedding from a circular cylinder. J. Fluids Struct. 10, 965–970.
Tensi, J., Boue, I., Paille, F., Dury, G., 2002. Modification of the wake behind a circular cylinder by using synthetic jets. J. Vis. 5, 37–44.
Thomas, F., Kozlov, A., Corke, T., 2008. Plasma actuators for cylinder flow control and noise reduction. AIAA J. 46 (8), 1921–1931.
Thomas, F.O., Kozlov, A., Corke, T.C., Plasma actuators for landing gear noise control, Journal of Fluids and Structures, 2005. In: Proceedings of the 11th AIAA/CEAS Aeroacoustics Conference Monterey, California.
Tokumaru, P.T., Diimotakis, P. E., 1989. Rotary oscillation control of a cylinder wake. In: Proceedings of the AIM 2nd Shear Flow Conference, March 13–16, 1989, 1 Tempe, AZ.
Valipour, M.S., Rashidi, S., Masoodi, R., 2014a. Magnetohydrodynamics flow and heat transfer around a solid cylinder wrapped with a porous ring. ASME J. Heat Transf. 136, 062601–062609.
Valipour, M.S., Rashidi, S., Bovand, M., Masoodi, R., 2014b. Numerical modeling of flow around and through a porous cylinder with diamond cross section. Eur. J. Mech. B/Fluids 46, 74–81.
Vilaplana, G., Grandemange, M., Gohlke, M., Cadot, O., 2013. Global mode of a sphere turbulent wake controlled by a small sphere. J. Fluids Struct. 41, 119–126.
Vit, T., Ren, M., Travnicek, Z., Marsik, F., Rindt, C.C.M., 2007. The influence of temperature gradient on the Strouhal–Reynolds number relationship for water and air. Exp. Therm. Fluid Sci. 31, 751–760.
Warjito, H.B., Kosasih, E.A., Tarakka, R., Simanungkalit, S.P., Made Fredy Lay Teryanto, I.G., 2012. Modification of flow structure over a van model by suction flow control to reduce aerodynamics drag, Makara, Teknol, 16, pp. 15–21.
Warui, H.M., Fujisawa, N., 1996. Feedback control of vortex shedding from a circular cylinder by cross-flow cylinder oscillations. Exp. Fluids 21, 49–56.
Weickgenannt, A., Monkewitz, P.A., 2000. Control of vortex shedding in an axisymmetric bluff body wake. Eur. J. Mech. B/Fluids 19, 93–104.
Weier, T., Gerbeth, G., 2004. Control of separated flows by time periodic Lorentz forces. Eur. J. Mech. B/Fluids 23, 835–849.
Weier, T., Gerbeth, G., Mutschke, G., Platacis, E., Lielausis, O., 1998. Experiments on cylinder wake stabilization in an electrolyte solution by means of electromagnetic forces localized on the cylinder surface. Exp. Therm. Fluid Sci. 16, 84–91.
Williams, J.E.F., Zhao, B.C., 1989. The active control of vortex shedding. J. Fluids Struct. 3 (2), 115–122.
Williamson, C.H.K., 1996. Vortex dynamics in the cylinder wake. Annu. Rev. Fluid Mech. 28, 477–539.
Williamson, C.H.K., Govardhan, R., 2004. Vortex-induced vibrations. Annu. Rev. Fluid Mech. 36, 413–455.
Wolfe, D., Ziada, S., 2003. Feedback control of vortex shedding from two tandem cylinders. J. Fluids Struct. 17, 579–592.
Wu, H., Sun, D.P., Lua, L., Teng, B., Tang, G.Q., Song, J.N., 2012. Experimental investigation on the suppression of vortex-induced vibration of long flexible riser by multiple control rods. J. Fluids Struct. 30, 115–132.
Xu, F., Chen, W.L., Xiao, Y.Q., Li, H., Ou, J.P., 2014. Numerical study on the suppression of the vortex-induced vibration of an elastically mounted cylinder by a traveling wave wall. J. Fluids Struct. 44, 145–165.
Zang, Z.P., Gao, F.P., 2014. Steady current induced vibration of near-bed piggyback pipelines: configuration effects on VIV suppression. Appl. Ocean Res. 46, 62–69.
Zang, Z.P., Gao, F.P., Cui, J.S., 2013. Physical modeling and swirling strength analysis of vortex shedding from near-bed piggyback pipelines. Appl. Ocean Res. 40, 50–59.
Zdravkovich, M.M., 1981. Review and classification of various aerodynamic and hydrodynamic means for suppressing vortex shedding. J. Wind Eng. Ind. Aerodyn. 7, 145–189.
Zhang, H., Fan, B., Chen, Z., Li, Y., 2014. Numerical study of the suppression mechanism of vortex-induced vibration by symmetric Lorentz forces. J. Fluids Struct. 48, 62–80.
Zhang, M.M., Cheng, L., Zhou, Y., 2004. Closed-loop-controlled vortex shedding and vibration of a flexibly supported square cylinder under different schemes. Phys. Fluids 16, 1439–1448.
Zhou, B., Wang, X., Gho, W.M., Tan, S.K., 2015. Force and flow characteristics of a circular cylinder with uniform surface roughness at subcritical Reynolds numbers. Appl. Ocean Res. 49, 20–26.
Zhu, H., Yao, J., 2015. Numerical evaluation of passive control of VIV by small control rods. Appl. Ocean Res. 51, 93–116.